Title

Advances in understanding the molecular basis of the first steps in color vision.

Authors

Hofmann, Lukas

Palczewski, Krzysztof

Publication Date

2015-11-01

DOI

10.1016/j.preteyeres.2015.07.004

Peer reviewed

HHS Public Access

Author manuscript

Prog Retin Eye Res. Author manuscript; available in PMC 2015 November 18.

Published in final edited form as:

Prog Retin Eye Res. 2015 November ; 49: 46–66. doi:10.1016/j.preteyeres.2015.07.004.

Advances in understanding the molecular basis of the first steps in color vision

Lukas Hofmann[*] and **Krzysztof Palczewski**[*]

Department of Pharmacology and Cleveland Center for Membrane and Structural Biology, School of Medicine, Case Western Reserve University, 10900 Euclid Avenue, Cleveland, OH 44106, USA

Abstract

Serving as one of our primary environmental inputs, vision is the most sophisticated sensory system in humans. Here, we present recent findings derived from energetics, genetics and physiology that provide a more advanced understanding of color perception in mammals. Energetics of *cis–trans* isomerization of 11-*cis*-retinal accounts for color perception in the narrow region of the electromagnetic spectrum and how human eyes can absorb light in the near infrared (IR) range. Structural homology models of visual pigments reveal complex interactions of the protein moieties with the light sensitive chromophore 11-*cis*-retinal and that certain color blinding mutations impair secondary structural elements of these G protein-coupled receptors (GPCRs). Finally, we identify unsolved critical aspects of color tuning that require future investigation.

Keywords

Color vision; Cone photoreceptor(s); Visual pigments; Spectral tuning; Energetics; Color blindness; Vision; Retina

1. Introduction

Color vision provides the primary human sensory perception of our environment and its understanding requires input from a variety of scientific fields (Bowmaker, 2008). It is initiated when photons of light penetrate the eye to reach the retina causing ‘excitation and photoisomerization’ of the 11-*cis*-retinylidene moieties bound to opsin proteins. Photoactivation of these visual GPCRs starts a series of enzymatic reactions collectively termed phototransduction (Polans et al., 1996; Ridge et al., 2003; Yau and Hardie, 2009). Photopigments represent an exclusive class of receptor proteins that cannot be activated by a classic molecular ligand (Kefalov, 2012; Orban et al., 2014; Palczewski, 2006; Rieke and Baylor, 1998; Salon et al., 2011). Instead, photopigments contain a prosthetic group, 11-*cis*-retinal, that once photoisomerized must be continuously regenerated to maintain vision *via* the retinoid cycle (termed in the past as visual cycle) (Kiser et al., 2014; Palczewski, 2012;

[*]Corresponding authors. Department of Pharmacology, School of Medicine, Case Western Reserve University, 10900 Euclid Avenue, Cleveland, OH 44106, USA. lxh278@case.edu (L. Hofmann), kxp65@case.edu (K. Palczewski).

Conflicts of interest

The authors have declared that no conflict of interest exists.

von Lintig et al., 2010). Thus, understanding how light interacts with nature's most sophisticated receptors – GPCRs – represents a unique scientific challenge. The phototransduction pathways within rods and cones are similar. In principle these pathways are designed on a common strategy involving homologous gene products with similar functions that significantly differ in some properties such as visual pigments sensitivities to light and their regeneration, kinetics and regulation of the reactions they initiate (reviewed in (Imai et al., 2005; Imamoto and Shichida, 2014; Kefalov, 2012; Korenbrot, 2012; Luo et al., 2008; Wang and Kefalov, 2011)). Moreover, vision is the major sensory perception system in various species, which makes it a favored target for comparative anatomy. In this review we address several topics of current interest in the first steps in color vision. These include the energetic aspects, disease phenotypes of color vision, and a comparative analysis of the organization of visual color receptors in different species.

2. Terminology and phylogeny of human cone visual pigments

2.1. Background

Visual pigments consist of different proteins called opsins and a universal chromophore 11-*cis*-retinal (Nathans, 1999; Stenkamp et al., 2002). The visual system of vertebrates encompasses five evolutionarily distinct classes of visual pigments: rhodopsin (Rh1), LWS, MWS (or Rh2), SWS1 and SWS2. Whether and how melanopsin contributes to vision is a topic of current research (Barrionuevo and Cao, 2014; Horiguchi et al., 2013; Schmidt et al., 2014b). All bind to the universal chromophore, 11-*cis*-retinal *via* a Schiff base, thus the difference in absorption originates from the different opsin protein moiety. Vertebrate photopigments contain glutamate as a primary counter anion in their third transmembrane sequence at position 113 to stabilize the protonated Schiff base (Collin, 2004; Jacobs, 2009; Nathans, 1999). Invertebrate visual pigments contain Y113 or F113 and a primary counter ion at position E181 in the second extracellular loop (ECL2). (Ramos et al., 2007; Terakita et al., 2004, 2000). The Rh1 class consists of rhodopsins responsible for scotopic vision. Phylogenetic analyses based on amino acid sequences revealed that the Rh1 class evolved from an ancestral short wavelength sensitive cone pigment about 540 million years ago (Bowmaker, 2008; Collin et al., 2003; Okano et al., 1992; Peichl, 2005). The other four classes known as cone pigments are responsible for photopic vision. Cone visual pigments are categorized according to both their maximum wavelengths of light absorption (λ_{max}) with bound chromophore and amino acid sequences: long wavelength sensitive (LWS) pigments absorb at a λ_{max} of 500–570 *nm*, medium wavelength sensitive (MWS or Rh2) pigments absorb at a λ_{max} of 480–530 *nm* and two short wavelength sensitive (SWS1, SWS2) pigments absorb at a λ_{max} of 354–445 *nm* and a λ_{max} of 400–470 *nm*, respectively (Hunt et al., 2009; Jacobs, 2008; Yokoyama, 2008).

2.2. Unique photoreceptor physiology improves color perception

Rod and cone photoreceptors form a unique blend of these cells in the retina. Comparison among different species revealed that the organization of the retina and photoreceptor cells varies as much as the species themselves (Walls, 1942). For instance, the ratio between rod and cone cells in nocturnal species is about 200:1 whereas it is about 20:1 in diurnal species (Peichl, 2005). Furthermore, expression of two different classes of opsins, SWS and either

MWS or LWS in one photoreceptor cell is an exclusive feature found in the house mouse, guinea pig and rabbit (Rohlich et al., 1994). SWS photopigments are unique cone pigments localized at the autosomal loci of their genes and they display the highest variability among species with respect to both their organization within the retina and their absorption maxima ranging from 360 nm for the SWS type 1 (SWS1) to 420 nm for the SWS type 2 (SWS2) pigment (Hunt and Peichl, 2014). The ability to tune 11-*cis*-retinal over such a broad range is due to several factors including the variable protonation state of the retinylidene moiety (Lewis et al., 2000; Nathans, 1990; Terakita et al., 2004). Furthermore, oil droplets, a special feature, are found in photoreceptor cells of birds, turtles, lizards, some fish and *Marsupialia* (Ahnelt et al., 1996; Arrese et al., 1999; Hannover, 1840). Oil droplets supposedly improve the quality of vision by increasing the signal to noise ratio, color contrast and hue discrimination (Vorobyev, 2003). This improved sensitivity is also maintained by a number of carotenoids located in oil droplets that absorb light at specific wavelengths (Goldsmith et al., 1984; Hart et al., 2006; Ives et al., 1983; Knott et al., 2010; Fischer, 1984).

2.3. Properties of trichromacy

Trichromatic vision implies the ability to detect light with three independent receptors differing in their wavelength sensitivities. Differences in λ_{max} between human long wavelength sensitive (L/LWS) and human medium wavelength sensitive (M/LWS) cone pigments improve distance-dependent discrimination between young and mature leaves, leaves and fruits, or ripe and unripe fruits (Bompas et al., 2013; de Lima et al., 2015; Dominy and Lucas, 2001; Matsumoto et al., 2014; Melin et al., 2014; Regan et al., 2001). Improved detection and selection of nutrients contributes further to an evolutionary advantage. Others have proposed an advantage of color vision can be found in the faster recognition and better memorization of colored things (Bredart et al., 2014; Gegenfurtner and Rieger, 2000; Wichmann et al., 2002). Environmental factors and nocturnal living habits have fostered a reduction from four to three classes of cone photopigments in mammals including humans (Bowmaker, 2008). Humans carry the Rh1 rhodopsin gene, as do all mammals, along with two variants of LWS cone opsin genes: the L/LWS and M/LWS cone opsin genes responsible for long wavelength and medium wavelength absorption. A third opsin encoded by the SWS1 gene is needed to attain trichromacy (Hunt et al., 2009; Nathans, 1999). Further, the three cone photopigments with their distinct sensitivities can match the visible spectrum by combination of three colors, namely red, green and blue (Fig. 1). An opposing processing theory of color vison is another physiological model which takes into account that certain pairs of colors cannot be seen together, e.g. red and green or blue and yellow (Fig. 2) (Dacey, 1996; Lee, 2014; Rowe, 2002). Electrophysiological recordings support the idea that responding neurons of the lateral geniculate nucleus can be divided into four wavelength-dependent groups. These groups are characterized according to the opposing system: +Red −Green, +Green −Red, +Blue −Yellow and +Yellow −Blue (Fig. 2) (De Valois et al., 1966). Besides these two theories of trichromacy and opponent colors, recent findings suggest the contribution of a fourth pigment – melanopsin – at high photopic levels to peripheral vision (Horiguchi et al., 2013; Schmidt et al., 2014b), and perhaps fifth, rod photoreceptor cells contribute to color vision (Barrionuevo and Cao, 2014). Current issues relating to color vision with an emphasis of neuronal processing are reviewed by (Lee, 2014).

Thus, colors play a major role in communication within and between species and can be considered a first primitive universal language. Communicating through colors can be a rapid, beautiful, meaningful, and subtle way of interaction. For instance, colors and color perception are crucial in avoidance of predators (camouflage), mimicry, warning or improving the chances of mating to assure successful reproduction and survival (Bloch, 2015; Jacobs and Nathans, 2009; Sandkam et al., 2015; Yokoyama, 2000).

3. Interplay of photoreceptors and neurons in color vison

Visual perception begins when photons of different energies interact with chromophores in distinct types of photoreceptor cells (Kefalov, 2012; Rieke and Baylor, 1998). These interactions transform the electromagnetic information into an electrochemical potential which then is modified, conducted and analyzed *via* different types of neurons (De Valois et al., 1966; Luo et al., 2008; Schmidt et al., 2014a). Color vision *per se* is processed by interconnected neurons, because the cone photoreceptor cells themselves are ‘colorblind’. A simple fact is that in scotopic vision the environment appears as black and white, although rod photoreceptor cells have their maximal sensitivities in the green spectral region (Fig. 1) (Lee, 2014; Schmidt et al., 2014a; Stockman, 2010). In the following paragraphs, we focus on the interplay of light with pigments and how neurons shape our color perception.

3.1. Multichromacy and its dimensions

Three cone photoreceptor types, each designated according to the opsin gene expressed, mediate human color vision. Thus, short wavelength sensitive cones contain SWS1 pigment, medium wavelength sensitive cones contain M/LWS pigment, and long wavelength sensitive cones contain L/LWS pigment. The wavelength of maximum absorption is around 420 nm for human SWS1 cones, near 530 nm for human M/LWS cones, and about 557 nm for human L/LWS cones (Dartnall et al., 1983; Merbs and Nathans, 1992; Neitz and Neitz, 2011; Stockman et al., 1993; Yoshizawa, 1994). Due to the spectral sensitivity of these three pigments and neuronal processing, humans can discriminate colors in the visible range of light from about 420 nm to 680 nm (Figs. 1–2, Tables 1 and 2) (Jacobs and Nathans, 2009). Aside from trichromatic vision, there also is di–, or tetrachromatic vision. Tetrachromatic vision, for example, is found in chickens and pigeons that possess an additional UV-sensitive photoreceptor besides the three usual photoreceptor types (Bowmaker, 1984; Vorobyev et al., 1998; Yoshizawa, 1994). The dimensionality of chromatic vision is not directly correlated with the number of pigment classes. Indeed, the presence of four cone classes does not implement tetrachromacy *per se*; only behavioral studies could reveal this correlation (Bowmaker, 2008). Albeit that the *mantis shrimp* has 12 types of photoreceptor cells ranging from ultraviolet (UV) to deep red, these 12 photoreceptor cell types do not indicate dodecachromacy. However, this shrimp certainly can absorb a broader spectrum of light than other species with less photoreceptors (Marshall and Oberwinkler, 1999). Recent, behavioral studies on the *mantis shrimp* showed that its color perception differs from the known human color opponent theory. Further, the 12 photoreceptors allow the *mantis shrimp* to detect colors more quickly. Thus the advantage lies in color detection rather than color discrimination (Land and Osorio, 2014; Thoen et al., 2014).

3.2. Neuronal contribution to color perception

Color vision and all other sensory perceptions are processed and evaluated by numerous neurons (Bowmaker, 2008). About 37% (or up to 60% depending on the literature source) of the human striate cortex is involved in the evaluation of only 3% of the visual field (Horton and Hoyt, 1991; Pahlberg and Sampath, 2011; Tolhurst and Ling, 1988; Wong and Sharpe, 1999). By comparing the number of involved neurons per sensory process, it becomes obvious that visual stimuli provide the most information about our environment. Post-photoreceptor signaling plays a major role in the discrimination and processing of visual stimuli (Bitensky et al., 1985; Conway et al., 2010; Dacey et al., 1996; De Valois and De Valois, 1993; Lee, 2014; Mancuso et al., 2010; Neitz and Neitz, 2011; Schmidt et al., 2014a; Stockman, 2010). The three-stage Müller zone model or the multi-stage color model by De Valois and De Valois provide a simplified and still controversial hypothesis of signal processing initiated by photoreceptors (De Valois and De Valois, 1993; Mancuso et al., 2010; Müller, 1930). Current models of color vision emphasize inputs from three types of cone photoreceptor cells and rod photoreceptor cells, which also contribute to daylight vision in the retina (Barrionuevo and Cao, 2014; Barrionuevo et al., 2014). Here rod photoreceptor cells elicit a light intensity-dependent signal modulated by horizontal cells (Szikra et al., 2014). Positing that stimuli elicited by rods and cones are modified by each other along neuronal pathways suggests that color vision results from more than a complex interplay between cone photoreceptor cells and other neurons (Barrionuevo and Cao, 2014; Barrionuevo et al., 2014; Conway et al., 2010; De Valois and De Valois, 1993; Dunn et al., 2007; Szikra et al., 2014). A revised model (Fig. 2) of the opponent color theory by De Valois and De Valois is provided by (Schmidt et al., 2014a). It states that cone opponent signals are processed through midget ganglion cells, where signals from cones are combined with those from horizontal cells. Thereby the ON/OFF state of bipolar cells and the SWS1 cone input play a major role in the transmission of the hue sensations yellow, blue, green and red. Based on this model, four hue mechanisms are proposed: yellow, L − (S + M); blue, (S + M) − L; green, M − (S + L); and red, (S + L) − M (Fig. 2) (Schmidt et al., 2014a). Melanopsin signaling can contribute to the contrast sensitivity in vision (Schmidt et al., 2014b). A model based on principal component analysis suggests how rod photoreceptor and ganglion cells containing melanopsin contributions could be achieved. In this principal component analysis, the most important chromatic contribution is also the blue–yellow input (Barrionuevo and Cao, 2014). How these signals from cone, rod photoreceptor cells and melanopsin-containing ganglion cells are processed and if the current models of color perception need to be expanded remain topics of ongoing research.

4. Energetics of *cis–trans* isomerization of 11-*cis*-retinal

In the following paragraphs, we focus on the energetics of *cis–trans* isomerization of 11-*cis*-retinal triggered by interaction with photons of specific energy (Barlow et al., 1993; Frutos et al., 2007; Gozem et al., 2012; Luo, 2000; McBee et al., 2001; Polli et al., 2010). Moreover, we discuss which physicochemical properties limit the visible spectrum and how these can be overcome.

To comprehend the principles of spectral tuning it is crucial to consider the mechanism of photoactivation from an energetic perspective. Photoactivation by a single photon generally leads to the same outcome, namely excitation of the chromophore and subsequent photoisomerization of retinal from 11-*cis*-retinal to the all-*trans*-configuration (Frutos et al., 2007; Gozem et al., 2012; Luo et al., 2008; Polli et al., 2010). To understand the activation by photons of different wavelengths or energies, it is critical to determine how the energetics vary with different interactions of the retinoid chromophore with its local environment. Such interactions form the basis of spectral tuning. Hence, characterizing the energetics of these interactions provides insights into how visual pigments accomplish the absorption of a wide UV–visible-IR spectrum of light with the same retinal chromophore, which by itself can only absorb light in the UV range (Fujimoto et al., 2009; Okada et al., 2002; Rajamani et al., 2011). Considering the process of photoactivation from an interdisciplinary perspective reveals the limitations that energetics and physiology impose on color perception at an early stage, where light passes through the cornea, lens, vitreous and ultimately interacts with the chromophore in the retina. Thus activation of visual pigment proteins requires breakage of a π bond. A minimal energy of $E_a^I \sim 156.4 \frac{kJ}{mol} \left(37.4 \frac{kcal}{mol}\right)$ in rhodopsin or $E_a^I \sim 61.8 \frac{kJ}{mol} \left(14.8 \frac{kcal}{mol}\right)$ in solution must be provided to break the π bond and cause isomerization (Dilger et al., 2015a; Luo, 2000). This energy level limits the visual spectrum on the IR side. Furthermore, the reduced transmission of UV-light by mostly the lens and cornea and to a lesser extent by the vitreous limits our light absorption on the short wavelength side of the spectrum and also protects the retina from radiation damage (Ambach et al.,1994; Norren and Vos, 1974; Walls, 1942). The human lens starts transmitting 50% of light at a wavelength range of 425–475 nm (Kessel et al., 2010; Lei and Yao, 2006). This 50% light transmission decreases with age and shifts towards 575 nm (Artigas et al., 2012; Dillon et al., 1999; Kessel et al., 2010). Further, cornea and aqueous humor show a more complex light transmission after 1300 nm with two declines at ~1400 nm and ~2000 nm. Moreover, the vitreous humor transmission shows two declines at ~1000 nm and ~1200 nm (Boettner and Wolter, 1962; van den Berg and Spekreijse, 1997). Thus the combined absorption by cornea, aqueous humor, lens and vitreous humor shapes the range of electromagnetic spectra of visual perception in humans.

4.1. Molecular insights into spectral tuning

11-*cis*-Retinal is the universal chromophore responsible for absorbing light in all four types of photoreceptors and melanopsin with the opsin and bound chromophore specifying the wavelength of absorbed light (Kiser et al., 2014). This unprotonated chromophore has an absorption maximum at about 380 nm in methanol solution and undergoes a bathochromic shift (towards longer wavelengths) upon protonation or covalent binding (Schiff base formation) (Blatz and Liebman, 1973; Fujimoto et al., 2005; Sakmar, 2012). Moreover, electrostatic interactions between the retinylidene moiety and the opsin protein environment cause additional tuning of wavelength absorption (Coto et al., 2006a, b; Zhou et al., 2014). These interactions include the pigments' different amino acid residues and also their spatial orientation, internal water molecules and counter ions. Overall covalent and non-covalent interactions of the bound retinal are responsible for the bond length alterations and

conformations of the chromophore crucial for fine-tuning spectral absorption (Coto et al., 2006b; Fujimoto et al., 2009; Okada et al., 2002; Rajamani et al., 2011). Thus, binding to amino acid residues, waters or counter ions that increase electron delocalization and decrease bond length alternation induce a bathochromic shift, whereas decreased electron delocalization and increased bond length alternation cause a hypsochromic shift (towards shorter wavelength) of the chromophore (Fujimoto et al., 2006; Sekharan et al., 2012). From a quantum chemical perspective a bathochromic or hypsochromic shift results from the relative stabilization of the excited electronic state (S_1) of the retinal chromophore with respect to the ground state (S_0). The electronic structure (charge distribution) of the excited state and ground state are different. Therefore, interactions that stabilize the charge distribution of the S_1 with respect to the charge distribution of the S_0 will cause a bathochromic shift. The same is true for a stabilization or destabilization of the S_0 with respect to the S_1 (Melaccio et al., 2012). Because no cone pigment structure is yet available, it is difficult to predict the coordinates of protein residues, counter anion hydrogen bond networks or waters to determine exactly how nature achieves specific spectral tuning for color vision. All our structural information about cone pigments (Stenkamp et al., 2002; Teller et al., 2003) is derived from modeling studies based on the rhodopsin structure (Palczewski et al., 2000).

All five photopigments including melanopsin have their maximal absorption (λ_{max}) at a unique wavelength. These maxima were measured and determined over decades by several groups using different methodologies (Asenjo et al., 1994; Bailes and Lucas, 2013; Bowmaker and Dartnall, 1980; Brown and Wald, 1964; Carroll et al., 2002; Dartnall et al., 1983; Merbs and Nathans, 1992; Oprian et al., 1991). The data reveal that there is a natural variation in λ_{max} caused predominantly by mutations in the 2, 3 and 4 exons of L/LWS and M/LWS opsin genes in normal color vision. Here we report a summary of currently available absorption maxima and calculate the energies of the specific wavelengths shown (Tables 1 and 2, and Fig. 1). Throughout this review we will refer to the λ_{max} values published by (Neitz and Neitz, 2011).

4.2. Physicochemical limits of human visible spectra

A photopigment is activated with a quantum yield of 0.65 when a photon of an electromagnetic wave with energy close to the absorption maximum strikes the chromophore (Kefalov et al., 2003; Kim et al., 2001, 2003; Liu and Colmenares, 2003; Rieke and Baylor, 1998). Measurements of absolute thresholds in human vision revealed that a single photon cannot provoke a physiological response. Absolute thresholds for humans to detect a signal through cones and rods are about 200 and 50 photons, respectively (Koenig and Hofer, 2011). A visual stimulus is elicited when the energy of a photon meets the energy required to promote the chromophore from an electronic ground state (S_0) to the first electronically excited singlet state (S_1) where it undergoes *cis–trans* isomerization to the photoproduct. Such photoisomerization involves the passage through a S_0/S_1 conical intersection that can be found along a plot of the energetics of the reaction (Barlowet al., 1993; Frutos et al., 2007; Gozem et al., 2012; Polli et al., 2010). Body temperature contributes continuously to the vibrational mode of the electronic ground state of the chromophore and thus destabilizes the ground state (Fig. 3) (Ala-Laurila et al., 2004; Luo et

al., 2011). QM/MM calculations of the excitation energies on free retinal in the gas phase range from $\Delta E_{S0\rightarrow S1}=197.8\frac{kJ}{mol}\left(47.3\frac{kcal}{mol}\right)$ to $232.5\frac{kJ}{mol}\left(55.6\frac{kcal}{mol}\right)$. The calculations of the chromophore in solution resulted in higher values because solvents stabilize S_0 relative to S_1, $\Delta E_{S0\rightarrow S1}=205.5\frac{kJ}{mol}\left(49.1\frac{kcal}{mol}\right)$ to $284.6\frac{kJ}{mol}\left(68.0\frac{kcal}{mol}\right)$ (Bravaya et al., 2007). The energy barrier for isomerization of the free retinal protonated Schiff-base chromophore was determined to be: $E_a^I=61.8\frac{kJ}{mol}\left(14.8\frac{kcal}{mol}\right)$, and the corresponding wavelength was λ = 1937.3 nm (Dilger et al., 2015b). Conversely, the energy barriers for chromophore isomerization in rhodopsin are higher compared to the free chromophore. Thus, they suggest that the pigment proteins restrict isomerization and thereby regulate sensitivity (Bravaya et al., 2007; Dilger et al., 2015a; Lorenz-Fonfria et al., 2010; Sugihara et al., 2002). The existence of an isomerization barrier stands in contrast to the barrier-free *cis–trans* isomerization as noted earlier by (Barlow et al., 1993; Frutos et al., 2007; Polli et al., 2010). Different activation energies are reported for the thermal activation path ranging from $E_a^T=91.63\frac{kJ}{mol}\left(21.9\frac{kcal}{mol}\right)$ to $200.96\frac{kJ}{mol}\left(48.03\frac{kcal}{mol}\right)$ (Baylor et al., 1980; Guo et al., 2014; Luo et al., 2011), and for the photochemical activation path from $E_a^P=188\frac{kJ}{mol}\left(45\frac{kcal}{mol}\right)$ to $240.21\frac{kJ}{mol}\left(57.41\frac{kcal}{mol}\right)$ (Barlowet al.,1993; Cooper, 1979; Gozem et al., 2012; Lorenz-Fonfria et al., 2010). The range of activation energy can be explained by different calculation models or protonation states of the chromophore. Thus, deprotonation leads to destabilization of the ground state thereby lowering the energy barrier for isomerization (Barlow et al., 1993). Others suggest that the difference of activation energy is due to conformational fluctuations of the binding pocket rather than the chromophore (Lorenz-Fonfria et al., 2010). Conformational fluctuations would further support the model of a different thermal-dependent isomerization mechanism controlled by an energy barrier E_a^T (Frutos et al., 2007; Gozem et al., 2012; Polli et al., 2010). An example of a deprotonated chromophore can be found in the UV pigment (SWS1) of the Siberian hamster. The thermal activation energy of UV pigment (SWS1) from a Siberian hamster is only half that of bovine rhodopsin (depending on the literature), about $96.3\frac{kJ}{mol}\left(23.0\frac{kcal}{mol}\right)$, which corresponds to λ = 1243.1 nm (Mooney et al., 2015). This result appears counter intuitive because the UV pigment (SWS1) is triggered by photons of higher energy than rhodopsin. Therefore, a higher activation energy would be expected for UV pigments. The reason for the higher thermal activation energy of rhodopsin lies in its increased photosensitivity compared to that of cone pigments. Whether the different sensitivity between the SWS1 photopigment and bovine rhodopsin only depends on the protonated state or if there are other factors, is part of ongoing research. The interdependence of the activation energy and maximal absorption in different photopigments is addressed by the Stiles Lewis–Barlow hypothesis that includes the thermal activation energy (E_a^T) as a constant which depends on the photon energy and thus the maximal absorption such as $E_a^T=const.\times\frac{1}{\lambda_{max}}$, *or const.* × λ_{max} (Barlow, 1957; Lewis, 1955; Stiles, 1948).

Spectroscopic and electrophysiological measurements combined with statistics indicate that E_a^T does not show a strict dependence on λ_{max} or on $\frac{1}{\lambda_{max}}$ for all pigments (Ala-Laurila et al., 2003, 2004; Koskelainen et al., 2000). Nevertheless, recent findings generated by quantum mechanical calculations showed that E_a^T of bovine rhodopsin indeed depends on $1/\lambda_{max}$, which supports an “anti-Barlow” correlation (Dilger et al., 2015a; Gozem et al., 2012). Thus, the interplay between the activation energy and absorption maxima is still a topic of debate. Only a combined approach of structural biology, computational chemistry and photochemistry will provide us further insight into the energetics of nature's photoreceptors.

From a pure energetic perspective based on bond dissociation, and neglecting the photochemical reaction path described above, the isomerization of 11-*cis*-retinal to all-*trans*-retinal requires breakage of a π bond. This C, C–π bond dissociation energy at the 11 and 12 position of the rhodopsin complex was stated to be $156.4 \pm 6.3 \frac{kJ}{mol} \left(37.4 \pm 1.5 \frac{kcal}{mol}\right)$, with the corresponding wavelength λ = 764.5 nm (Luo, 2000). The thermal isomerization of the chromophore in rhodopsin, supposedly proceeds by a different path as its photoactivation requires an activation energy of about $E_a^T \sim 146 \frac{kJ}{mol} \left(35 \frac{kcal}{mol}\right)$, with the corresponding wavelength λ = 819.0 nm (Gozem et al., 2012). Both wavelengths also relate to the energetic minimum of the human visible spectrum. Thus, it remains to be answered if cone photopigments also participate in two activation routes, both through a λ_{max} specific photoactivation path and a photopigment universal thermal activation path. Moreover, the maximal energy limit of the human visible spectrum is about 380 nm which is $314.6 \frac{kJ}{mol} \left(75.2 \frac{kcal}{mol}\right)$. With this amount of energy, it is possible to break weak C–H or C–C single bonds (Luo, 2000). Breakage of a C–C or C–H bond would lead to a decay of the chromophore or other macromolecules which would harm the retinoid cycle and thus impair vision (Kiser et al., 2014). However, the lens and vitreous show a higher absorption of short wavelength light that prevents damage to the retina by high energy irradiation (Norren and Vos, 1974). These data provide a physicochemical explanation for the natural limits of the human visual spectrum. However, a recent publication about IR vision indicates that these limits can be extended by two-photon isomerization with modern instruments. Thereby, the two-photon effect enables detection of IR light emitted by a laser (Palczewska et al., 2014).

4.3. The interplay of light and heat on the activation energy

Studies about the interplay of light and heat in bovine rhodopsin revealed that the thermal activation energy (E_a^T) showed an increased temperature dependence $E_a^T = 202.8 \frac{kJ}{mol} \left(48.5 \frac{kcal}{mol}\right)$ for wavelengths beyond 590 nm. Conversely, no thermal contribution was needed at wavelengths shorter than 590 nm (St George, 1952). The activation energy above 750 nm corresponds to the thermal activation energy of bovine rhodopsin mentioned above. Taken together, the thermal activation energy of bovine

rhodopsin lies between $E_a^T = 91.63 \frac{kJ}{mol} \left(21.9 \frac{kcal}{mol}\right)$ and $200.96 \frac{kJ}{mol} \left(48.03 \frac{kcal}{mol}\right)$ (Baylor et al., 1980; Guo et al., 2014; Luo et al., 2011; Lythgoe and Quilliam, 1938) and the photochemical activation energy $E_a^P = 188 \frac{kJ}{mol} \left(45 \frac{kcal}{mol}\right)$ to $240.21 \frac{kJ}{mol} \left(57.41 \frac{kcal}{mol}\right)$ (Barlow et al., 1993; Cooper, 1979; Gozem et al., 2012; Lorenz-Fonfria et al., 2010; Luo et al., 2011; St George, 1952). A further indication of a higher E_a^T is shown by two different toad rhodopsins, where different E_a^T values of $185.4 \frac{kJ}{mol} \left(44.3 \frac{kcal}{mol}\right)$ and $204.2 \frac{kJ}{mol} \left(48.8 \frac{kcal}{mol}\right)$ were observed despite their similar absorption spectra (Ala-Laurila et al., 2002). A recent *in vitro* experiment revealed an unusual temperature dependence of E_a^T for bovine rhodopsin based on a rearrangement of the hydrogen network within the retinal–binding pocket. At a temperature of 310.15 K (37 °C), $E_a^T = 92.0 \frac{kJ}{mol} \left(22.0 \frac{kcal}{mol}\right)$ and at 317.15 K (44 °C), $E_a^T = 477.0 \frac{kJ}{mol} \left(114.0 \frac{kcal}{mol}\right)$ (Guo et al., 2014). The reported differences in E_a^T between (Ala-Laurila et al., 2002) and(Guo et al., 2014) are due to the different decay models used. The latter takes into account that thermal decay of rhodopsin measured at 500 nm consists of both the thermal isomerization and hydrolysis of the Schiff base (Liu et al., 2011, 2009). Furthermore, basic Boltzmann statistics were used to describe the thermal activation of a complex molecule such as retinal. Basic Boltzmann statistics reduce a complex reaction to a simple process like the collision of gas molecules (Luo et al., 2011). Thus, the use of basic Boltzmann statistics and conventional Arrhenius analysis contribute further to the difference found between the above stated activation energies. Furthermore, the lipidic environment of rhodopsin changes at higher temperatures and thus should influence the decay of rhodopsin (Garavito and Ferguson-Miller, 2001; Paleologos et al., 2005; Stalikas, 2002; Vautier-Giongo and Bales, 2003). Recent findings reveal that the isomerization of the chromophore is an exclusive mechanism for thermal activation (Yanagawa et al., 2015). Further, they found a relationship between the thermal stability of rhodopsin, the low dark noise and the stability of the activated Meta II state (Yanagawa et al., 2015). Discrepancies between theoretical activation energies of 11-*cis*-retinal isomerization and minor deviance from experimental energies indicate that the mathematical models are improving; however, they are still a matter of controversy in the fields of computational chemistry, photochemistry and biochemistry, thus much remains to be answered.

4.4. Human vision beyond the visible spectra

Human rhodopsin sensitivity was calculated and measured at 1050 nm ($114.0 \frac{kJ}{mol}$, or $27.2 \frac{kcal}{mol}$) (Griffin et al., 1947). These calculations based on classic Maxwell–Boltzmann distribution suggested that rhodopsin bleaches and absorbs light even at 1050 nm and with $10^{-12.4}$ times less sensitivity than at 510 nm (Griffin et al., 1947; St George, 1952). Moreover, *in vitro* investigations revealed that the relative sensitivity at long wavelengths

increases upon warming and also shifts λ_{max} to shorter wavelengths (Ala-Laurila et al., 2003). The threshold of the activation energy $184.1\frac{kJ}{mol}\left(44.0\frac{kcal}{mol}\right)$ at 1050 nm ($114.0\frac{kJ}{mol}$, or $27.2\frac{kcal}{mol}$) can be achieved with the addition of thermal energy provided from the human physiological temperature of 310.15 K (37 °C) $\left(72.3\frac{kJ}{mol}, 16.8\frac{k\mathrm{cal}}{mol}\right)$ (Fig. 3). However, this activation requires $10^{12.4}$ more photons due to the reduced sensitivity of bovine rhodopsin at 1050 nm (St George, 1952). Fig. 3 shows the combinations of thermal energy (red bars) and quantum energy (blue bars) at various wavelengths. The thermal energy contribution facilitates activation from 675 nm to 1050.9 nm where the quantum energy of light would not suffice to achieve the threshold of activation energy (black line). Recent findings demonstrate that mammalian photoreceptors can elicit a signal if irradiated with IR light at wavelengths longer than 800 nm (Palczewska et al., 2014). Here excitation is triggered by a two-photon effect yielding a total energy corresponding to twice the single photon energy (Fig. 1). Thus, doubling the energy leads to a color perception corresponding to one photon in the visual spectra. Although this multi-photon excitation is a remarkable observation, the extent to which this two-photon excitation shapes our visual perception remains to be determined.

4.5. Phototransduction noise of photoreceptor cells

Phototransduction noise of photoreceptor cells determines our visual sensitivity (Aho et al., 1988; Angueyra and Rieke, 2013; Bulmer et al., 1957). Phototransduction noise originates from two sources; one is the thermal noise of visual pigments, the other results from phototransduction downstream events. Thus, the extent to which each source contributes to this noise depends on both the photoreceptor cell and photopigment type (Angueyra and Rieke, 2013; Kefalov, 2012; Korenbrot, 2012; Rieke and Baylor, 2000). In addition to significant structural differences between rods and cones (Mustafi et al., 2009), cone photoreceptor cells bear an increased noise compared to rod photoreceptor cells (Barlow, 1957; Rieke and Baylor, 2000; Yanagawa et al., 2015). A comparison of phototransduction noise events in salamander long wavelength sensitive (LWS) and short wavelength sensitive (SWS) cone photoreceptor cells revealed that in LWS cones the noise is mainly caused by spontaneous activation of the photopigment (thermal noise), whereas in SWS cones downstream events are responsible for the phototransduction noise (Rieke and Baylor, 2000). A comparison of primate cone photoreceptor cells suggests that phototransduction noise in cone photoreceptor cells is dominated by noise from downstream events such as channel noise and fluctuations in cGMP concentrations and not by thermal noise (Angueyra and Rieke, 2013; Fu et al., 2008). The thermal noise of visual pigments is determined by the energetic states of the chromophore or structural fluctuations of the binding pocket and ultimately shapes the spectral sensitivity of each photoreceptor cell (Aho et al., 1988; Gozem et al., 2012; Lorenz-Fonfria et al., 2010; Rinaldi et al., 2014). Recent work determined two key residues E122 and I189 in rhodopsin which contribute to the lower dark noise compared to cone visual pigments (Yanagawa et al., 2015). The source of noise that contributes to the photoreceptor sensitivity is still a topic of ongoing research.

5. Molecular insights into color tuning

5.1. Molecular insights into SWS1 color tuning

The human SWS1 cone pigment induces a hypsochromic shift in the absorption maximum of 11-*cis*-retinal, with a published peak absorption of human SWS1 cone pigment ranging from 410 to 450 nm (Tables 1 and 2 and Fig. 1) (Asenjo et al., 1994; Bowmaker and Dartnall, 1980; Brown and Wald, 1964; Dartnall et al., 1983; Merbs and Nathans, 1992; Neitz and Neitz, 2011; Oprian et al., 1991). Several investigations combining site-directed mutagenesis, spectroscopy, modeling, quantum mechanics/molecular mechanics (QM/MM) estimates and combinations of these approaches have provided insights into the molecular mechanism of spectral tuning by SWS1 cone pigment.

The low 62% identity in protein sequence between rhodopsin and SWS1 opsin indicates a difference in intramolecular interactions despite a similar function. Highly conserved residues and domains within visual pigments suggest their crucial role in function including color tuning. For instance, conserved in human cone pigments, the F207 residue plays an important role in photoactivation and a minor role in spectral tuning. Replacing F207 with a V, Y, T or S consistently leads to a reduction or absence of absorption without changing λ_{max} (Kuemmel et al., 2013). Moreover, a less conserved acidic residue in visual pigments in ECL2 D181 or E181 plays a crucial role in GPCR activation as a counter ion switch (Terakita et al., 2004, 2000; Yan et al., 2003). Thereby, GPCR activation causes a proton transfer from E181 to E113 through a hydrogen bond network resulting in the activated GPCR conformation (Martinez-Mayorga et al., 2006; Ramos et al., 2007; Yan et al., 2003). However, the M/LWS and L/LWS photopigments do not contain an acidic residue at position 181, but an H197 residue which serves as chloride-binding site (Wang et al., 1993; Yan et al., 2003). If and how the chloride ion contributes to the activation mechanism as the above mentioned acidic residues D181 and E181 remains to be answered. Furthermore, sequence alignments of the visual pigments showed seven conserved residues in ECL2: R177, P180, G182, S186, C187, G188, and D190 (rhodopsin numbering). These residues, though preserved, can play different roles in SWS1 and other visual pigments. Mutational and molecular dynamic (MD) studies of *Xenopus* violet cone pigment, a SWS1 class opsin, revealed a hydrogen bonding network between ECL2, ECL3 and the N-terminus. Despite the conserved residues in ECL2, bovine rhodopsin's ECL2 shows extensive interactions between ECL3 and the N-terminus *via* a hydrogen network without direct interactions with ECL3 or the N-terminus. Finally, mutagenesis studies revealed that E176 and S181 participate in protein folding and chromophore binding in *Xenopus* violet cone pigment (Chen et al., 2011). The differences at the N-terminal (extracellular) domain between cone pigments and rhodopsin provide a possible explanation for the increased chromophore dissociation. Cone visual pigments show a dark dissociation comparable to 500 photoisomerizations per s (Kefalov et al., 2005). A more open conformation of the extracellular domains allow small nucleophilic agents to penetrate the binding site and cause hydrolysis of the chromophore (Wald et al., 1955). Moreover, the SWS1 pigment Meta II state decays 40 times faster than rhodopsin, despite their similar photoresponses. This effect could also originate from reduced cone pigment stability (Kefalov et al., 2003; Shi et al., 2007). According to QM/MM calculations, the molecular basis of spectral tuning within the

UV to violet wavelength range involves stabilization of either the deprotonated (UV) or protonated (violet) Schiff base. Deprotonation increases bond length alternation and thus causes a hypsochromic shift of 11-*cis*-retinal absorption (Altun et al., 2011, 2009; Zhou et al., 2014). Additional structural modeling, QM/MM calculations and mutagenesis studies indicated that a complex hydrogen network forms an inter-helical lock within TM2, TM3 and TM6. This lock contributes to stabilization of the deprotonated Schiff base and thus enables the spectral tuning of Siberian hamster UV cones (Sekharan et al., 2013). Mutagenesis studies showed that a single amino acid substitution, S90C, is responsible for the major hypsochromic shift of 34–46 nm in avian SWS1 pigment and, further supporting this observation, the C90S reverse substitution, caused a bathochromic shift of 38 nm in zebra finch. However, similar mutagenesis studies of mouse and bovine SWS1 pigments indicate that the S90C substitution showed only a marginal effect, whereas a single substitution at position F86Y was responsible for their 70 nm difference in absorbance (Sekharan et al., 2013; Yokoyama et al., 2000). Despite difficulties with interpretation, mutagenesis studies of photopigments combined with evaluation of their changes in absorption are a powerful approach. We must remember that a mutation without an effect on absorption could still change the hydrogen bond network if, for example, waters rearrange in the binding pocket and compensate for the changed residue. Thus it is difficult to draw conclusions about spectral tuning from mutagenesis studies alone.

These results indicate that spectral tuning in different cone pigments and species is maintained by complex interactions involving different amino acids. Therefore, each cone opsin class from different species must be examined individually. Also, spectral tuning results from a complex interplay between multiple amino acid residues, hydrogen bond networks and waters within the chromophore-binding site. A combined approach of mutagenesis studies and QM/MM modeling would shed a new light on the mechanisms of spectral tuning.

5.2. Molecular insights into color tuning of M/LWS and L/LWS cones

Both M/LWS and L/LWS cone photopigment induce a bathochromic shift in the absorption maximum of 11-*cis*-retinal relative to free retinal. Published absorption peaks of these cone visual pigments range from 552 to 563 nm and 525–533 nm, respectively (Tables 1 and 2 and Fig. 1) (Asenjo et al., 1994; Bowmaker and Dartnall, 1980; Brown and Wald, 1964; Dartnall et al., 1983; Merbs and Nathans, 1992; Neitz and Neitz, 2011; Oprian et al., 1991). Several approaches including mutagenesis, spectroscopy, modeling studies, and their combinations have yielded insights into the molecular mechanisms of spectral tuning by M/LWS and L/LWS cone pigments.

Alignment of the human L/LWS and M/LWS protein sequences displays a difference in a total of fifteen amino acids. Of these fifteen, seven amino acids are responsible for the spectral difference between human L/LWS and M/LWS cone pigments as determined by Oprian's group. Listed from L/LWS to M/LWS, these amino acids are: S116Y, S180A, I230T, A233S, Y277F, T285A and Y309F (Fig. 4) (Asenjo et al., 1994). Other groups using mutagenesis found that five amino acids and their interactions are responsible for the spectral tuning between vertebrate LWS and Rh2 pigments: S180A, H197Y, Y277F,

T285A, and A308S (Wang et al., 1993; Yokoyama et al., 2008). Three of these five mutations are identical with the seven amino acids responsible for the spectral tuning in the L/LWS and M/LWS pigments. These data show that spectral tuning resulting in the same spectral shift can be accomplished through different combinations of amino acid substitutions. Fifteen implicated amino acids differ between L/LWS and M/LWS. Thus theoretically there are 15^{20} possible mathematical combinations that could achieve the spectral absorption of the human L/LWS and M/LWS by only considering the changes in standard amino acids. These results reinforce the conclusion that spectral tuning involves a set of highly complex interactions amongst different residues, chromophore and internal waters which cannot be derived accurately through mutagenesis alone. Furthermore, the LWS cone pigments harbor an additional feature for spectral tuning called the ‘chloride effect’ wherein a chloride-binding site located near His197 contributes to the bathochromic shift of retinal in both human L/LWS and M/LWS cone pigments (Wang et al., 1993; Yamashita et al., 2013). The same effect is found in iodopsin (chicken LWS pigment) wherein depletion of chloride leads to a hypsochromic shift of about 40 nm (Hirano et al., 2001). The ‘chloride effect’ has been reported in mouse visual pigments where it also accounts for the above mentioned hypsochromic shift (Sun et al., 1997). Moreover, this chloride effect causes a faster decay of the Meta I state and, thereby, a more rapid formation of the active state (Morizumi et al., 2012). Results published to date are derived from mutagenesis of different amino acids close to the chromophore and their impacts upon spectral tuning. Absorption of naturally occurring visual pigments illustrate the extensive repertoire of absorption spectra which nature maintains ranging from 355 nm in *Danio rerio* (Zebrafish) to 625 nm in *Anolis carolinensis* (American Chameleon) (Amora et al., 2008; Chinen et al., 2003; Kawamura and Yokoyama, 1993). An extreme example of artificial tuning was performed with human cellular retinol–binding protein II. Systematic mutagenesis of amino acids close to the chromophore led to absorption spectra ranging from 425 nm up to 644 nm (Sakmar, 2012; Wang et al., 2012). The described artificial spectral tuning through the cellular retinol-binding protein II gave insights into the correlation between electrostatic effects, counter anion, structure of 11-*cis*-retinal and absorbed wavelength (Huntress et al., 2013). An artificially engineered system such as this experiment demonstrates is the marked ability of 11-*cis*-retinal to absorb light over a broad spectrum. Yet it fails to provide further insights into how nature and evolution accomplish color tuning. Besides the role of amino acid residues in spectral tuning, investigations of rhodopsin revealed that internal waters play a crucial role in the hydrogen bonding network and thus in spectral tuning (Okada et al., 2002). Because cone photopigment crystal structures are lacking, the role of waters and the precise location of the hydrogen networks have yet to be documented. This fact reinforces the need for crystallographic structures for each human cone pigment to fully understand the molecular details underlying spectral tuning in cone photopigments.

6. Deficiencies in color vision

Inherited color vision deficiencies of various types and degrees occur in humans (Neitz and Neitz, 2011; Roosing et al., 2014). Among others, these include different types of monochromacy, the common red–green color deficiencies and blue–yellow color deficiency.

There are two forms of monochromacy: Form 1, rod monochromacy or achromatopsia; and Form 2, blue cone monochromacy or incomplete achromatopsia. Form 1 is caused by mutations in the CNGA3 gene, CNGB3 gene, GNAT2 gene, or PDE6C/H gene. Patients suffering from rod monochromacy caused by mutations in CNGA3 have normal rod and cone pigment levels but only rod responsivity (Alpern, 1974; Kohl et al., 2000, 2002, 1998). Mutations in the CNGB3 gene and the PDE6C gene alter the function of cones and also decrease the number of cone photoreceptors in the retina (Grau et al., 2011; Thiadens et al., 2009; Varsanyi et al., 2007). Form 2 is caused by mutations in the locus control region for the human long wavelength sensitive (L/LWS) and human medium wavelength sensitive (M/LWS) pigment genes or harmful mutations in both L/LWS and M/LWS genes which cause the absence of functional LWS cone pigments (Gardner et al., 2014, 2009, 2010; Mizrahi-Meissonnier et al., 2010; Nathans et al., 1989).

Red–green color deficiencies are largely due to increased non-homologous recombination of nearly identical sequences of L/LWS and M/LWS opsin genes. Gene duplication of the L/LWS gene lead to a head-to-tail array of numerous L/LWS and M/LWS genes. Numerous copies of L/LWS and M/LWS opsin genes in this array increase the probability of unequal crossing-over where one or more of the six exons are exchanged (Crognale et al., 1998; Deeb et al., 1992; Hayashi et al., 2006; Jagla et al., 2002; Nathans et al., 1986a; Neitz et al., 1989; Neitz et al., 1996). Successful gene therapy in red–green color blind primates shows that common color vision deficiency can be rescued. Thus, successful treatment of a non-human adult primate indicates that gene therapy in a neuronal context can be effectively applied after the developmental stage (Mancuso et al., 2009). Another proposed rescue of daylight vision has been achieved by cell transplantation in mice (Santos-Ferreira et al., 2015).

Blue–yellow color deficiency can be caused by one of the six known mutations or other unreported mutations within the human short wavelength sensitive (SWS1) opsin gene (Table 3) (Neitz and Neitz, 2011). Interestingly, none of the mutated amino acid residues interact directly with the chromophore or show a shift of the SWS1 pigment spectral sensitivity (Fig. 6). Only seven amino acid residues are responsible for the spectral shift between L/LWS and M/LWS pigment of which only three interact directly with the chromophore. This fact leads us to conclude that the six mutations in the SWS1 opsin must perturb the folding, hydrogen bond network, stability, activation or transport instead. One reason for the minor number of known mutations which shift the spectral absorption in the SWS1 pigment is that mutations causing a minor shift of the SWS1 pigment will not overlap with the absorption spectra of other visual pigments. Thus a mutation causing a spectral shift of the SWS1 pigment will not result in a severe compromising color vision deficiency and is not reported.

6.1. Tritanopia

SWS1 cones comprising about 6% of all human cones, are distributed independently throughout the retina and show a hexagonal packing with neighboring photoreceptor cells (Curcio et al., 1987; Hofer et al., 2005; Lombardo et al., 2013a,b). Tritanopia is a SWS1 cone-related disease. Humans suffering from tritanopia are unable to differentiate colors in

the middle to short wavelength region of the visible spectrum (Fig. 5). Such variations of spectral discrimination are due to amino acid substitutions in the SWS1 cone pigment. Compared to the 8% prevalence of red–green visual defects, the occurrence of tritanopia is much lower, affecting only 0.001%–0.2% of the human population (Gunther et al., 2006). Tritanopia also increases during aging as cones become less sensitive to light with a reduction affecting the sensitivity of SWS1 cones at least as much as that of L/LWS and M/LWS cones (Eisner et al., 1987; Johnson et al., 1988; Shinomori et al., 2001; Werner and Steele, 1988). The age-related loss of short wavelength sensitivity cannot or only partially be attributed to yellowing of the lens. A comparison study with younger tested persons showed that other factors such as pupil size, background illumination level, iris color and macular pigment density can account for the reduced perception (Beirne et al., 2008a,b). Another explanation, found by neurological studies on the SWS1 cone pathway, showed that a neural loss in the retinal circuit and lateral geniculate nucleus causes a delayed SWS1 cone OFF response and thus an altered sensitivity (Shinomori and Werner, 2012).

Genealogical studies have revealed that tritanopia is an autosomal dominant trait with incomplete penetrance, whereas protanopia and deuteranopia involve the X-chromosome and thus exhibit an X-linked pattern of inheritance (Krill et al., 1971; Smith et al., 1973; Wright, 1952). Six disease-causing mutations are known to cause tritanopia: L56P, G79R, T190I, S214P, P264S and R283Q (Table 3) (Baraas et al., 2007, 2012; Gunther et al., 2006; Weitz et al., 1992a,b). As illustrated in Fig. 6, these mutations do not interact with the chromophore itself. However, replacement of a rigid nonpolar Pro residue, with a polar or a charged residue or *vice versa* can distort the overall protein structure, impair GPCR activation or transport, all of which result in the loss of blue–yellow color perception (Weitz et al., 1992a,b; Zalewska et al., 2014). The point mutation R283Q in the SWS1 opsin was shown to be associated with progressive SWS1 cone degeneration, analogous to the rod degeneration seen in retinitis pigmentosa (Baraas et al., 2007).

6.2. Red–green color deficiency

Individuals suffering from red–green color deficiencies possess only two fully functional cone pigments, namely SWS1 and either M/LWS or L/LWS. The loss of functional L/LWS photopigment results in protanopia, whereas a shifted absorption of L/LWS photopigment causes protanomaly. The loss of functional M/LWS pigment results in deuteranopia, whereas a shifted absorption of M/LWS pigment causes deuteranomaly (Fig. 5). Non-homologous recombination or point mutations within the L/LWS or M/LWS opsin genes produce these deficiencies (Fig. 5) (Deeb, 2004; Neitz and Neitz, 2011). The spectral separation between the impaired L/LWS and M/LWS pigments determines the severity of the color vision defect. The small difference ($\Delta_{M/LWS\ L/LWS}$ = 27.5nm) in spectral absorption between human L/LWS and M/LWS pigments is crucial for correct red–green color vision. A spectral shift of about 5 nm caused by the S180A mutation accounts for 18% of the total wavelength difference between L/LWS and M/LWS. A shift of 5 nm in the absorption of the SWS1 cone pigment would only account for 4.5% or 3.6% of the total absorption difference between SWS1 and M/LWS or L/LWS, respectively. Thus mutations that cause a minor shift in the SWS1 pigment will cause a smaller change in color perception compared to shifts in M/LWS or L/LWS pigment absorption (Pokorny et al., 1981).

The L/LWS and M/LWS opsin genes are located in a head-to-tail tandem array on the human X-chromosome (Fig. 7) (Nathans et al., 1986b). The amino acid sequence identity between L/LWS and M/LWS opsins is 96%, and they have only 42% and 43% identity with the SWS1 opsin and rhodopsin (Nathans et al., 1986b; Okano et al., 1992). The number of copies and sequences of both the L/LWS and M/LWS opsin genes varies among people with normal color vision (Fig. 7) (Neitz and Neitz, 1995; Yamaguchi et al., 1997). For example, the L/LWS opsin exists as two prominent Ser/Ala variants at position 180 in humans with normal color vision which differ in λ_{max} by about 4 nm (Neitz and Jacobs, 1986). The high degree of inherited red–green color vision deficiency (~8%) can be explained by a high frequency of unequal homologous recombination (McClements et al., 2013; Roosing et al., 2014). The high frequency of recombinations is promoted by the high homology of the L/LWS and M/LWS opsins. Non-homologous pairing, gene conversion and unequal cross-overs within this tandem array result in color vision deficiencies of different severity such as protanopia, protanomaly, deuteranpia, deuteranomaly or blue-cone monochromacy (Figs. 5 and 7) (Deeb, 2004; Neitz and Neitz, 2011). Transcription of both the L/LWS and M/LWS opsins is regulated *via* a 3.5 kb upstream locus control region (LCR) (Nathans et al., 1989; Wang et al., 1992). Therefore, the 5′-first and the 5′-second of numerous LWS opsin genes are transcribed and regulated by this LCR (Fig. 7) (Carroll et al., 2002; Deeb, 2005; McMahon et al., 2008; Winderickx et al., 1992a; Yamaguchi et al., 1997). Deletion or damage of the LCR results in blue-cone monochromacy (BCM) (Figs. 5 and 7) (Nathans et al., 1989).

6.3. L/LWS-M/LWS genetics

The L/LWS and M/LWS genes consist of six exons, one more (the first exon) than the rhodopsin and SWS1 genes that contain only 5 exons (Nathans et al., 1986b). Exon five of the L/LWS and M/LWS opsins is primarily responsible for the spectral differences in light absorption (Neitz and Jacobs, 1986). Because L/LWS and M/LWS opsin genes are located on the X-chromosome, females are theoretically capable of tetrachromacy. Addition of one more dimension within the visible spectra to trichromacy fails to produce a significant phenotypic advantage for these carriers (Jordan et al., 2010).

To date, several point mutations are known which result in red–green color deficiencies (Table 3). Some of these are summarized in (Carleton et al., 2005). Three different mutational mechanisms were categorized into three classes. First, deletion of the LCR; second, missense mutation in an LWS hybrid gene; and third, an exon 3 single-nucleotide polymorphism (Gardner et al., 2014). Here we report a selection (N94K, R247Ter, C203R, P307L, R330Q and G338E) of known class two and three mutations in L/LWS and M/LWS opsins and their corresponding disease phenotypes. All of these missense mutations result in either the absence of expression or lack of function of the corresponding photopigment. Males who have an X-chromosome opsin gene array in which there is a single gene containing one of these missense mutations, will experience blue cone monochromacy. In contrast, a male with two or more opsin genes on the X-chromosome in which one of the first two genes contains one of these missense mutations will be a dichromat. The type of dichromacy, protan or deutan, depends on whether the mutation is in the L/LWS opsin gene (protan) or M/LWS opsin gene (deutan). The point mutation G338E in L/LWS or M/LWS

opsin results in a protan or deutan dichromacy, respectively, because of the inactivated photopigment (Ueyama et al., 2002). The mutation N94K, C203R or P307L in either L/LWS or M/LWS results in a lack of light absorption and thus in dichromacy (Nathans et al., 1993; Reyniers et al., 1995; Ueyama et al., 2002). The mutation R330Q found in M/LWS causes deutan dichromacy because of reduced absorption at 530 nm (Ueyama et al., 2002). The mutation R247Ter in a male with only a single LWS gene leads to blue-cone monochromacy due to an early stop codon after the fifth transmembrane helix (Nathans et al., 1993; Reitner et al., 1991). Furthermore, a deleterious combination of polymorphisms involving amino acids L153, I171, A174, V178 and A180 (LIAVA) can result in protanopia, deuteranopia or even blue-cone monochromacy (Fig. 5) if present in both L/LWS and M/LWS genes (Carroll et al., 2004; Crognale et al., 2004; Gardner et al., 2014; Mizrahi-Meissonnier et al., 2010; Ueyama et al., 2012). Besides LIAVA, the two single nucleotide polymorphisms leading to amino acid combinations of LVAVA and MIAVA were recently found to cause aberrant splicing (Gardner et al., 2014; Ueyama et al., 2012).

X-linked cone dystrophy is yet another and more severe color vision deficiency. Here opsin dysfunction causes degeneration primarily of cone photoreceptors and subsequently rod photoreceptors resulting in severely impaired vision. Cone dystrophy differs from cone-rod dystrophy in that intact peripheral vision is retained in the former. Point mutations W177R and C203R in the third and fourth exon of the L/LWS- and M/LWS-genes are known to cause progressive X-linked cone dystrophy. Both mutations cause aggregation and accumulation of opsins within the endoplasmic reticulum of human neuroblastoma cells, similar to the rhodopsin retinitis pigmentosa-causing mutation P23H (Dryja et al., 1990; Gardner et al., 2010). Compared to P23H rhodopsin, the W177R mutation cannot be rescued with 9-*cis*-retinal (Gardner et al., 2010). Moreover, the linkage disequilibrium between LIAVA and W177R supports the concept of abundant gene conversions between the two homologous L/LWS and M/LWS opsin genes (Gardner et al., 2010).

6.4. Transcription regulation of L/LWS and M/LWS opsin genes

Epigenetic studies have shown that rod and cone opsin transcription is regulated by several mechanisms, including interactions of at least three photoreceptor-specific transcription factors at the promoter or coding regions and looping of the *cis*-regulatory region LCR or rhodopsin enhancer region (RER) (Fig. 7). The latter interaction decreases as the distance increases between the LCR or RER and the promoter or coding region (Fig. 7). The three transcription factors are the cone-rod homeobox (CRX), the neural retina leucine zipper (NRL), and nuclear receptor subfamily 2, group E, member 3 (NR2E3) (Peng and Chen, 2011). GTF2IRD1 is an additional transcription factor found in human and mouse retina that might regulate the level and topology of rod and cone photoreceptor gene expression as well as the three known transcription factors (Farkas et al., 2013; Masuda et al., 2014). Understanding transcription regulation mechanisms could increase the probability of transcribing fully functional copies of either an L/LWS or M/LWS gene and thereby restoring color vision in individuals with impaired color perception (Cideciyan et al., 2013). Recent advances in somatic cell research revealed that fully functional photoreceptor cells derived from induced fibroblasts can further up-regulate the endogenous *NRL* and *NR2E3* genes required for photoreceptor cell specification (Seko et al., 2014). Furthermore,

successful transplantation of cone-like photoreceptors into mouse retinas with cone degeneration demonstrates the therapeutic potential of stem cell and gene therapies to cure these visual diseases (Dalkara et al., 2015; Santos-Ferreira et al., 2015). Notably, restoration of color vision in a red–green color blind primate also emphasizes the potential of gene therapy (Mancuso et al., 2009). Furthermore, genetic deletion of both SWS gene alleles slowed down cone photoreceptor cell degeneration in a Leber congenital amaurosis mouse model. This finding implies that a combinatorial approach of gene therapy and pharmacological chaperones that improves folding of cone visual pigments should slow down photoreceptor degeneration (Zhang et al., 2015).

7. Color vision among species

The retina is a highly specialized light sensor that can detect chromatic, spatial and temporal variations in light. This nerve tissue has also evolved adaptively to the particular environment of an animal's habitat (Ahnelt and Kolb, 2000; Bloch, 2015; Peichl, 2005; Szel et al., 1994a). Thus, an animal possesses color vision if it can discriminate between stimuli that differ in their distributions of spectral energy. Or more precisely, it needs to possess: a) photoreceptors with distinct photopigments, and b) a neuronal circuit which connects the outputs of these receptors with the central nervous system (Jacobs, 1993). The most sophisticated visual sensory system is found in the cones of sauropsids. Aside from several differing visual pigments and types of cone cells, they possess double cones, cone photoreceptor cells containing two outer segments with two different visual pigments such as LWS or RH2, and pigmented oil droplets that serve as chromatic filters. These features permit tetrachromatic vision and further improve hue and contrast discrimination (Ahnelt and Kolb, 2000; Vorobyev, 2003; Vorobyev et al., 1998). Varying ratios of cone and rod cells between different species indicate an environmentally-related sculpting of the retina which influences the numerical ratio and also the structures of rod and cone photoreceptor cells. Adaptation of the first mammals to nocturnal activity led to a rod-dominated retina which affected photoreceptor cells and subsequently also the organization of second-order neurons (Ahnelt and Kolb, 2000; Hart et al., 2006; Peichl, 2005).

In 1840, Adolph Hannover discovered colored oil droplets in bird cone photoreceptor cells (Hannover, 1840). Almost 100 years later Gordon Lynn Walls reported the presence of an oil droplet located before the disc membranes of cones or rods in a variety of species including sturgeon, marsh hawk, leopard frog, snapping turtle, western painted turtle, and marbled lungfish (Walls, 1942). The presence of these oil droplets in cone photoreceptor cells of all birds, and some reptiles, amphibians, mammals and fish was later confirmed by several other groups (Fischer, 1984; Robinson, 1994; Vorobyev, 2003). The presence of an oil droplet in just a minority of various species suggests that this feature could be an ancient feature of visual cells. Genealogical studies dated the origin of colored droplets to about 400 million years ago. That pigmented oil droplets are found exclusively in tetra or higher chromatic species indicates that they provide an advantage only when many different photopigment types are present (Robinson, 1994). Walls and Hannover noted that some oil droplets in cones contain dissolved yellow, orange or red pigments (Table 4) (Hannover, 1840; Walls, 1942). Light absorption by these oil droplets varied from 375 to 477 nm depending on their pigments.

Analysis of extracted pigments showed that these were carotenoid derivatives, such as astaxanthin, zeaxanthin or ε-carotene (Goldsmith et al., 1984). Further information about carotenoids and a structural perspective about their enzymatic cleavage was reviewed by (Sui et al., 2013). Some droplets contained up to two carotenoid pigments. Avian oil droplets have been classified based on their spectrophotometric and morphological properties (Table 4) (Goldsmith et al., 1984). Because pigmented oil droplets absorb light at specific wavelengths, they could enhance color contrast, acting as filters to exclude certain wavelengths of light. An additional function could be protection against damage by light in the short wavelength range (Goldsmith et al., 1984; Hart et al., 2006; Fischer, 1984). Calculations of energy distribution indicate that oil droplets enhance the absolute sensitivity at one wavelength and also the signal-to-noise ratio of photoreceptor cells through absorption of scattered photons in the retina (Ives et al., 1983). In contrast, absorption of any wavelength of light in a dim lit environment would be disadvantageous. A study of pigmented oil droplets in chicken retina showed that the carotenoid density was proportional to the light intensity of their environment. This finding indicates that the visual pigment density and therefore the absorption could be adapted on a seasonal timescale to optimize color perception (Hart et al., 2006). Furthermore, the dietary uptake of carotenoids can modify the composition and concentration of carotenoids found in avian oil droplets (Knott et al., 2010). Taken together, the features of colored or non-colored oil droplets probably improve both color–contrast and hue discrimination. This improvement could be highly beneficial, especially where colors play a crucial role in natural selection (Vorobyev, 2003; Vorobyev et al., 1998).

Through all the species the light absorbing prosthetic group in visual pigments is a retinal analog or retinal (Urich, 2013). So far four different visual chromophores were characterized; Retinal (RAL_1) is the universal chromophore found in most vertebrates and invertebrates (Wald, 1939a, b). Porphyropsin, 3-dehydroretinal (RAL_2) is found in fish, some amphibians and reptiles (Allison et al., 2004; Suzuki et al., 1984a; Toyama et al., 2008; Wald, 1939b). Those two chromophores (RAL_1 and RAL_2) compete for the same binding site in opsin proteins if present in photoreceptor cells (Allison et al., 2004; Suzuki et al., 1984b). Xanthopsin, 3-hydroxyretinal (RAL_3) was exclusively discovered in the visual system of insects and occurs in two enantiomeric forms (3R and 3S) (Kirschfeld et al., 1977; Seki and Vogt, 1998; Vogt and Kirschfeld, 1983). 4-Hydroxyretinal (RAL_4) the forth chromophore was discovered in firefly squid (Matsui et al., 1988). A comparison of RAL_2 and RAL_1 in salamander red rods demonstrated that RAL_1 improves dark noise levels compared to RAL_2 (Ala-Laurila et al., 2007). The origin and further advantages besides the peak absorption of the different chromophores $RAL_{1–4}$ in visual pigments is not fully understood.

7.1. Variations of cone photoreceptor organization throughout species

When immunohistochemistry is used to compare mammalian retinas, the largest diversity of cone abundance is found in rodents. This finding is not surprising, as rodents constitute the most species-rich order and occupy a large variety of habitats. Moreover, the distribution of cone photoreceptor cells is similar in the retinas of all mammalian species. The highest cone density is found in the dorsotemporal quadrant of the retina's *Area centralis* with a

centroperipheral density gradient. A search for SWS cones revealed either their absence in species such as whales, seals and some nocturnal species or a distribution similar to LWS or MWS cones. Notably, SWS cones account for only about 5–10% of total cones distributed into three regions: first, a centro-peripheral density gradient of SWS cones with a peak density at the *Area centralis* in the dorso-temporal quadrant; second, a high SWS cone concentration in the ventral retina, and third, a reverse topography of SWS cones with a high density in the peripheral retina and a low density in the central retina (Lukats et al., 2005; Peichl, 2005; Szel et al., 2000). Typically, photoreceptor cells contain only a single visual pigment in most species. Immunohistochemical analyses of the retina have revealed, however, that in some species that there are regions with dually pigmented cones co-expressing two pigments (Lukats et al., 2005). ERG studies in mice and Siberian hamsters revealed that dual cones are sensitive to UV and long wavelength light (Calderone and Jacobs, 1999; Jacobs et al., 2004). How these signals are processed and contribute to color perception is still unknown. Expression of two LWS and SWS opsins within one photoreceptor cell is a rare phenomenon in mammalian species. To date, such dually pigmented cones have been detected in the house mouse, guinea pig and rabbit (Rohlich et al., 1994). Dual cones first express the SWS opsin and then later in development express MWS and LWS opsins (Lukats et al., 2005; Szel et al., 1994b). The distribution of such pigmented cones throughout the retina differs among species. An interesting pattern is found in mice where SWS and LWS pigments are distributed along a dorsoventral gradient. In dorsal cones MWS and LWS opsins are preferentially expressed but in ventral cones, SWS opsin expression dominates. A high abundance of SWS pigments in the ventral region is also found in insectivores (Lukats et al., 2005). The function of these dually pigmented cells could serve more in broadband detection than in specific color contrast discrimination (Peichl, 2005).

7.2. SWS cones: a distinct member of the retina

The uneven distribution of SWS cones within the retina is not fully understood. However, the increased SWS cone density in the ventral retina region in species such as rodents implies an evolutionary adaption to blue skylight because that is the background from which their predators attack (Lukats et al., 2005; Peichl, 2005). Two-photon imaging, statistics and immunohistochemistry were used to investigate the response properties of MWS and SWS cones based on their loci in mouse retina. The results indicate that the improved detection of achromatic contrast in the sky region originates from a higher gain of SWS cones in the ventral retina, and not from greater spectral sensitivity (Baden et al., 2013). Further, lower phototransduction noise in photoreceptor cells leads to higher visual sensitivity (Aho et al., 1988; Angueyra and Rieke, 2013). SWS photopigments have reduced noise compared to most LWS photopigments, thus the improved detection could partially result from a lower phototransduction noise in SWS cone photoreceptor cells (Rieke and Baylor, 2000). An exceptional feature of SWS cones is their complete absence in the retinas of bottlenose dolphins. Also notable is a distribution of SWS cones found in the ground squirrel that differs from the pattern exhibited by LWS and MWS cones (Fig. 8). Loss of SWS cones can occur in distinct mammalian species, and loss of SWS cones is common in marine mammals. This observation seems counter intuitive as short wavelength light is the major source of light in open, clear water (Griebel, 2002). LWS and rod pigments of marine

mammals also exhibit a hypsochromic shift which possibly could compensate for their loss of SWS cones (Peichl, 2005; Peichl et al., 2001).

Humans and most primates have a cone-rich region in the retina termed the fovea which can be compared with the *Area centralis* of other mammals. Consisting of tightly packed cones, the fovea is almost devoid of rods (Fig. 9). Moreover, entering light can avoid crossing secondary neurons because these are bent away from the fovea (Provis et al., 2013). This morphology makes the fovea well suited for high resolution vision of focused objects. Photoreceptor cells are organized within a mosaic in the retina, their distribution varying from a completely random to an ordered hexagonal topography. A hexagonal organization represents the closest packing comparable to crystal packing, wherein one cone photoreceptor is surrounded by six photoreceptor cells. This highly ordered packing is prominently found with cones, whereas rods disrupt the hexagonal topography by having four to five directly neighboring photoreceptor cells (Ahnelt and Kolb, 2000; Lombardo et al., 2013a,b; Pum et al., 1990). Such an arrangement allows the highest density of light sensors and thus one of the highest possible optical resolutions in nature. Conversely, irregularities in cone photoreceptor organization found in their mosaics are mainly due to curvature, local noise, interference from other cellular subpopulations, and meridional changes of size and composition (Ahnelt, 1998; Hirsch J Fau - Miller and Miller, 1987). Such irregularities result in areas where one photoreceptor class is predominant or absent, and as a result, these regions will be more or less sensitive to one wavelength. In humans and some primates, the number of SWS cones is markedly reduced in the foveal pit. SWS cones have the highest density within the fovea around the foveal pit. Although the impact of this foveal organization is still unknown, it should be noted that short wavelength light is dispersed to a higher degree than medium or long wavelength light, depending on the wavelength-specific refractive index. This fact would explain why SWS cones are mainly located in the foveal ring surrounding the foveal pit (Ahnelt, 1998; Curcio et al., 1987; Lukats et al., 2005; Walls, 1942). Such foveal organization also compensates for the greater dispersion of short wavelength light through the cornea, lens and vitreous (Fig. 9). Furthermore, transmission of short wavelength light is reduced more than that of medium and long wavelength light. Dispersion plus transmission properties of the cornea and lens contribute to the explanation of why no SWS1 cone pigments are found in the center of the fovea and why SWS cones account for only 5–10% of all cone photoreceptor cells. The fovea contains increased concentrations of carotenoids that absorb short wavelength light (Hammond et al., 1997). Thus, the ability to absorb blue light indicates a scavenger effect similar to that found in oil droplets, which absorb scattered photons within the eye and thereby, improve the signal to noise ratio. Limited space in the retina has forced nature to build the most effective, efficient and sophisticated light sensors with minimal redundancy in the photoreceptor cell population (Fig. 9). As do all optical systems, the eye also suffers from chromatic anomalies depending on the wavelength of light. For example, short wavelengths exhibit greater deviations than long wavelength light resulting in myopia (near sightedness) for short wavelengths and hyperopia (far sightedness) for long wavelengths of light (Charman and Jennings, 1976). These abnormalities cause three optical effects, namely alterations in focus, position and magnification. The difference in focus stems from a longitudinal chromatic aberration, whereas differences in position and magnification are

based on transverse chromatic aberrations (TCA) (Fig. 9) (Gupta et al., 2010; Rucker and Osorio, 2008; Rynders et al., 1995). Herein we propose that the organization and distribution of photoreceptor cells within and around the fovea partially compensate for these abnormalities. Furthermore, neurons in the brain process visual stimuli and match them together to form a meaningful image (Artal et al., 2004; Ohlendorf et al., 2011; Sabesan and Yoon, 2010). Thus, organization of the fovea and processing through neurons compensate for the disruptive effects of chromatic aberrations. Besides the fovea, there is a cone-rich rim consisting of L/LWS and M/LWS cone photoreceptors found at the *ora serrata* of the human retina. This organization of cones could contribute to color perception by detecting dispersed light, although its function has not yet been fully established (Curcio et al., 1987; Mollon et al., 1998). Others propose three advantages for the band of cones at the edge of the retina with respect to peripheral vision. First, is to detect objects crossing the visual field based on a change in contrast. Second, cones can evoke a signal in bright daylight because they are not saturated under bright light conditions. Third, the time response of cones is more rapid than that of rods, allowing a faster and steady perception (Lamb, 2013; Williams, 1991). Measurements of color perception in the intermediate periphery confirmed the ability of peripheral red–green color detection (Hansen et al., 2009). How the cone-rich rim contributes to peripheral color perception remains to be answered. Müller glial cells can contribute to our color perception as shown by a combined experimental and computational experiments (Agte et al., 2011; Franze et al., 2007; Labin et al., 2014). Thus, these neurons act as wavelength-dependent wave guides to selectively direct incoming photons to corresponding cone- or rod- photoreceptor cells, a concept reminiscent of the passage of light through fiber optics. The idea of Müller glial cells as wave guides is controversial in the field of vision. Questions of how Müller glial cells might select specific wavelengths and thus improve light perception or if Müller glial cells simply degrade vision remain to be answered.

8. Conclusions

Here we provide an overview of the first steps in color vision by combining the most recent relevant information in the fields of physics, chemistry and biology. History has taught us that such an interdisciplinary combination can contribute substantially to our knowledge of this process. However future progress will require the incorporation of new approaches involving other disciplines as well to answer more complex scientific questions about light perception and the spectral tuning of cone pigments.

Visual perception starts with the absorption of photons, excitation of the chromophore and the *cis*-*trans*-isomerization of 11-*cis*-retinal in the retina and ends with signal processing in our central nervous system. Thus, vision and the perception of color is a highly complex process involving an interplay of photons, chromophore, opsin proteins, neurons and their crosstalk. Herein, we discuss energetic aspects along with chemical properties of the chromophore, which provide insights into the natural limits of our visible spectra. The physical properties of light and its dispersion through cornea, lens, and vitreous limit our color perception. Moreover, the distribution of LWS, MWS, and SWS cone photoreceptors throughout the retina seems to be shaped by evolution to optimize visual perception in the particular habitat of a species. The hypothesis that the organization of photoreceptor cells at

the fovea compensates for wavelength-dependent aberrations caused by the lens also seems likely. An exotic nonetheless effective device to optimize color perception is the oil droplet found in the retinas of birds, fish, reptiles and marsupials. Oil droplets supposedly improve contrast by filtering out unwanted wavelengths of light through absorption by carotenoids which further improves the signal-to-noise ratio. Similar carotenoids are found in retinas of mammals, especially at high concentrations in and around the fovea. Whether these carotenoids act as scavengers for scattered photons and thus have the same function as an oil droplet remains unknown.

Color vision deficiencies can be inherited or caused by various mutations or unequal crossovers, resulting in a reduced, shifted or absent wavelength sensitivity in at least one cone photopigment. To date, up to six point mutations in the SWS1 opsin are known to cause tritanopia, a deficiency in blue spectral sensitivity. The more frequent red–green color deficiency can be caused by various point mutations similar to tritanopia. Moreover, a major motif is found in the increased number of recombinants between the highly homologous L/LWS and M/LWS opsin genes. Transcription of these opsin genes is regulated by the LCR, such that deletion or mutation of the LCR leads to BCM. Furthermore, transcription of one of the numerous L/LWS or M/LWS opsin gene copies depends on the distance between LCR and the copy; thus the shorter this distance, the greater the transcription. Gene therapy can be used to cure red–green color blindness in adult primates (Mancuso et al., 2009). Moreover, how these findings can be applied to humans is a topic of current research interest.

Structural studies, computational chemistry, mutagenesis and biochemistry have provided insights into the spectral tuning of the universal chromophore, 11-*cis*-retinal. Nevertheless, we stress here that mutagenesis of single amino acids and spectral analyses do not take the complex interaction of internal visual pigment waters, hydrogen bond networks and their rearrangements into account. Thus, more experimental data at a molecular level are desperately needed to decipher the secrets of nature's spectral tuning.

9. Future directions

The highest resolution structures of cone pigments are urgently required to identify their side-chain arrangements and also to reveal water molecules and hydrogen bond networks that reside within the transmembrane bundles of GPCR helices. Such structures will demonstrate the multiple components that contribute to the spectral properties of visual pigments including: a) the organization of internal waters; b) protonation states of other pigment residues along with the helical bundles; and c) conformations and twisting of the chromophore within the binding pocket. To supplement this structural data, radiolytic footprinting methods should provide additional information about water interactions and movements. Moreover, cations and anions can significantly change the spectral tuning of visual pigments. These charged molecules need to be identified in the pigment structures and correlated with the corresponding spectra.

Combined X-ray crystallography, electron crystallography and radiolytic footprinting studies will provide details for cone pigments unprecedented in GPCR structural

determination. This information will constitute a platform for initiating molecular dynamics and quantum mechanics computational studies. Quantum mechanical calculations of the chromophore in the binding pocket will reveal the mechanism of spectral tuning for each of the cone pigments. Although such mechanisms have long been studied, direct observation and calculation will only be enabled with high-resolution structural data made possible through the multidisciplinary protocols outlined above. Hybrid QM/MM molecular dynamics trajectories will reveal structural changes that take place in the chromophore, the protein, and bound waters during the photochemical and thermal chromophore isomerization reaction.

Acknowledgments

We thank especially Drs. Leslie T. Webster, Jr., Maureen Neitz, Adam Smith and Massimo Olivucci for insightful comments on this manuscript. Additional comments from Drs. David T. Lodowski, Yoshikazu Imanishi, Paul S. Park, Johannes Von Lintig, John J. Mieyal, and members of the Palczewski laboratory were most helpful. This work was supported by funding from the National Institutes of Health EY009339 (KP), and Arnold and Mabel Beckman Foundation. L. H. is supported by the Swiss National Science Foundation Doc.Mobility fellowship (P1SKP3_158634). K.P. is John H. Hord Professor of Pharmacology.

Abbreviations

BCM	blue cone monochromacy
CR	cone-rod homeobox
ECL	extracellular loop
E_a^I	isomerization energy
E_a^T	thermal activation energy
E_a^p	photochemical activation energy
GPCR	G protein-coupled receptor
IR	infrared
LCR	locus control region
L/LWS	human red long wavelength sensitive
LWS	long wavelength sensitive
MD	molecular dynamics
M/LWS	human green long wavelength sensitive
MWS or Rh2	medium wavelength sensitive
NRL	neural retina leucine zipper
NR2E3	nuclear receptor subfamily 2, group E, member 3
PR	promoter region
QM/MM	quantum mechanics/molecular mechanics
RAL	retinal

RER	rhodopsin enhancer region
Rh1	rhodopsin
SWS1	short wavelength sensitive type 1
(S_1)	first electronically excited singlet state
(S_0)	ground electronic state
UV	ultraviolet

References

Agte S, Junek S, Matthias S, Ulbricht E, Erdmann I, Wurm A, Schild D, Kas JA, Reichenbach A. Muller glial cell-provided cellular light guidance through the vital guinea-pig retina. Biophys. J. 2011; 101:2611–2619. [PubMed: 22261048]

Ahnelt PK. The photoreceptor mosaic. Eye (Lond). 1998; 12(Pt 3b):531–540. [PubMed: 9775214]

Ahnelt PK, Kolb H. The mammalian photoreceptor mosaic-adaptive design. Prog. Retin Eye Res. 2000; 19:711–777. [PubMed: 11029553]

Ahnelt PK, Hokoc JN, Rohlich P. The opossum photoreceptors–a model for evolutionary trends in early mammalian retina. Rev. Bras. Biol. 1996; 56(Su 1 Pt 2):199–207. [PubMed: 9394501]

Aho AC, Donner K, Hyden C, Larsen LO, Reuter T. Low retinal noise in animals with low body temperature allows high visual sensitivity. Nature. 1988; 334:348–350. [PubMed: 3134619]

Ala-Laurila P, Saarinen P, Albert R, Koskelainen A, Donner K. Temperature effects on spectral properties of red and green rods in toad retina. Vis. Neurosci. 2002; 19:781–792. [PubMed: 12688672]

Ala-Laurila P, Albert RJ, Saarinen P, Koskelainen A, Donner K. The thermal contribution to photoactivation in A2 visual pigments studied by temperature effects on spectral properties. Vis. Neurosci. 2003; 20:411–419. [PubMed: 14658769]

Ala-Laurila P, Pahlberg J, Koskelainen A, Donner K. On the relation between the photoactivation energy and the absorbance spectrum of visual pigments. Vis. Res. 2004; 44:2153–2158. [PubMed: 15183682]

Ala-Laurila P, Donner K, Crouch RK, Cornwall MC. Chromophore switch from 11-cis-dehydroretinal (A2) to 11-cis-retinal (A1) decreases dark noise in salamander red rods. J. Physiol. Lond. 2007; 585:57–74. [PubMed: 17884920]

Allison WT, Haimberger TJ, Hawryshyn CW, Temple SE. Visual pigment composition in zebrafish: evidence for a rhodopsin-porphyropsin interchange system. Vis. Neurosci. 2004; 21:945–952. [PubMed: 15733349]

Alpern M. What is it that confines in a world without color? Invest. Ophthalmol. 1974; 13:648–674. [PubMed: 4605446]

Altun A, Yokoyama S, Morokuma K. Color tuning in short wavelength-sensitive human and mouse visual pigments: ab initio quantum mechanics/molecular mechanics studies. J. Phys. Chem. A. 2009; 113:11685–11692. [PubMed: 19630373]

Altun A, Morokuma K, Yokoyama S. H-bond network around retinal regulates the evolution of ultraviolet and violet vision. ACS Chem. Biol. 2011; 6:775–780. [PubMed: 21650174]

Ambach W, Blumthaler M, Schopf T, Ambach E, Katzgraber F, Daxecker F, Daxer A. Spectral transmission of the optical media of the human eye with respect to keratitis and cataract formation. Doc. Ophthalmol. 1994; 88:165–173. [PubMed: 7781484]

Amora TL, Ramos LS, Galan JF, Birge RR. Spectral tuning of deep red cone pigments. Biochemistry. 2008; 47:4614–4620. [PubMed: 18370404]

Angueyra JM, Rieke F. Origin and effect of phototransduction noise in primate cone photoreceptors. Nat. Neurosci. 2013; 16:1692–1700. [PubMed: 24097042]

Arrese C, Dunlop SA, Harman AM, Braekevelt CR, Ross WM, Shand J, Beazley LD. Retinal structure and visual acuity in a polyprotodont marsupial, the fat-tailed dunnart (Sminthopsis crassicaudata). Brain Behav. Evol. 1999; 53:111–126. [PubMed: 10085478]

Artal P, Chen L, Fernandez EJ, Singer B, Manzanera S, Williams DR. Neural compensation for the eye's optical aberrations. J. Vis. 2004; 4:281–287. [PubMed: 15134475]

Artigas JM, Felipe A, Navea A, Fandino A, Artigas C. Spectral transmission of the human crystalline lens in adult and elderly persons: color and total transmission of visible light. Invest. Ophthalmol. Vis. Sci. 2012; 53:4076–4084. [PubMed: 22491402]

Asenjo AB, Rim J, Oprian DD. Molecular determinants of human red/green color discrimination. Neuron. 1994; 12:1131–1138. [PubMed: 8185948]

Baden T, Schubert T, Chang L, Wei T, Zaichuk M, Wissinger B, Euler T. A tale of two retinal domains: near-optimal sampling of achromatic contrasts in natural scenes through asymmetric photoreceptor distribution. Neuron. 2013; 80:1206–1217. [PubMed: 24314730]

Bailes HJ, Lucas RJ. Human melanopsin forms a pigment maximally sensitive to blue light (lambda(max) approximate to 479 nm) supporting activation of G(q/11) and G(i/o) signalling cascades. Proc. R. Soc. B Biological Sci. 2013; 280

Baraas RC, Carroll J, Gunther KL, Chung M, Williams DR, Foster DH, Neitz M. Adaptive optics retinal imaging reveals S-cone dystrophy in tritan color-vision deficiency. J. Opt. Soc. Am. A Opt. Image Sci. Vis. 2007; 24:1438–1447. [PubMed: 17429491]

Baraas RC, Hagen LA, Dees EW, Neitz M. Substitution of isoleucine for threonine at position 190 of S-opsin causes S-cone-function abnormalities. Vis. Res. 2012; 73:1–9. [PubMed: 23022137]

Barlow HB. Purkinje shift and retinal noise. Nature. 1957; 179:255–256. [PubMed: 13407693]

Barlow RB, Birge RR, Kaplan E, Tallent JR. On the molecular origin of photoreceptor noise. Nature. 1993; 366:64–66. [PubMed: 8232538]

Barrionuevo PA, Cao D. Contributions of rhodopsin, cone opsins, and melanopsin to postreceptoral pathways inferred from natural image statistics. J. Opt. Soc. Am. A Opt. Image Sci. Vis. 2014; 31:A131–A139. [PubMed: 24695161]

Barrionuevo PA, Nicandro N, McAnany JJ, Zele AJ, Gamlin P, Cao D. Assessing rod, cone, and melanopsin contributions to human pupil flicker responses. Invest. Ophthalmol. Vis. Sci. 2014; 55:719–727. [PubMed: 24408974]

Baylor DA, Matthews G, Yau KW. Two components of electrical dark noise in toad retinal rod outer segments. J. Physiol. 1980; 309:591–621. [PubMed: 6788941]

Beirne RO, McIlreavy L, Zlatkova MB. The effect of age-related lens yellowing on Farnsworth-Munsell 100 hue error score. Ophthalmic Physiol. Opt. 2008a; 28:448–456. [PubMed: 18761482]

Beirne RO, Zlatkova MB, Chang CK, Chakravarthy U, Anderson RS. How does the short-wavelength-sensitive contrast sensitivity function for detection and resolution change with age in the periphery? Vis. Res. 2008b; 48:1894–1901. [PubMed: 18585404]

Bitensky MW, George JS, Whalen M, Yamazaki A. Molecular mechanisms of visual excitation - a concatenation of nonlinear cellular processes. J. S. tat. Phys. 1985; 39:513–541.

Blatz PE, Liebman PA. Wavelength regulation in visual pigments. Exp. Eye Res. 1973; 17:573–580. [PubMed: 4782841]

Bloch NI. Evolution of opsin expression in birds driven by sexual selection and habitat. Proc. Biol. Sci. 2015; 282:20142321. [PubMed: 25429020]

Boettner EA, Wolter JR. Transmission of the Ocular Media. Life Support Systems Laboratory, 6570th Aerospace Medical Research Laboratories, Aerospace Medical Division, Air Force Systems Command. 1962

Bollinger K, Sjoberg SA, Neitz M, Neitz J. Topographical cone photopigment gene expression in deutan-type red-green color vision defects. Vis. Res. 2004; 44:135–145. [PubMed: 14637363]

Bompas A, Kendall G, Sumner P. Spotting fruit versus picking fruit as the selective advantage of human colour vision. Iperception. 2013; 4:84–94. [PubMed: 23755352]

Bowmaker JK. Microspectrophotometry of vertebrate photoreceptors. A brief review. Vis. Res. 1984; 24:1641–1650. [PubMed: 6398563]

Bowmaker JK. Evolution of vertebrate visual pigments. Vis. Res. 2008; 48:2022–2041. [PubMed: 18590925]

Bowmaker JK, Dartnall HJ. Visual pigments of rods and cones in a human retina. J. Physiol. 1980; 298:501–511. [PubMed: 7359434]

Bravaya K, Bochenkova A, Granovsky A, Nemukhin A. An opsin shift in rhodopsin: retinal S0–S1 excitation in protein, in solution, and in the gas phase. J. Am. Chem. Soc. 2007; 129:13035–13042. [PubMed: 17924622]

Bredart S, Cornet A, Rakic JM. Recognition memory for colored and black-and-white scenes in normal and color deficient observers (dichromats). PLoS One. 2014; 9:e98757. [PubMed: 24879303]

Brown PK, Wald G. Visual pigments in single rods and cones of the human retina. Direct measurements reveal mechanisms of human night and color vision. Science. 1964; 144:45–52. [PubMed: 14107460]

Bulmer MG, Howarth CI, Cane V, Gregory RL, Barlow HB. Noise and the visual threshold. Nature. 1957; 180:1403–1405. [PubMed: 13493537]

Calderone JB, Jacobs GH. Cone receptor variations and their functional consequences in two species of hamster. Vis. Neurosci. 1999; 16:53–63. [PubMed: 10022478]

Carleton KL, Spady TC, Cote RH. Rod and cone opsin families differ in spectral tuning domains but not signal transducing domains as judged by saturated evolutionary trace analysis. J. Mol. Evol. 2005; 61:75–89. [PubMed: 15988624]

Carroll J, McMahon C, Neitz M, Neitz J. Flicker-photometric electroretinogram estimates of L: M cone photoreceptor ratio in men with photopigment spectra derived from genetics. J. Opt. Soc. Am. A Opt. Image Sci. Vis. 2000; 17:499–509. [PubMed: 10708031]

Carroll J, Neitz J, Neitz M. Estimates of L: M cone ratio from ERG flicker photometry and genetics. J. Vis. 2002; 2:531–542. [PubMed: 12678637]

Carroll J, Neitz M, Hofer H, Neitz J, Williams DR. Functional photoreceptor loss revealed with adaptive optics: an alternate cause of color blindness. Proc. Natl. Acad. Sci. U. S. A. 2004; 101:8461–8466. [PubMed: 15148406]

Charman WN, Jennings JA. Objective measurements of the longitudinal chromatic aberration of the human eye. Vis. Res. 1976; 16:999–1005. [PubMed: 948891]

Chen MH, Sandberg DJ, Babu KR, Bubis J, Surya A, Ramos LS, Zapata HJ, Galan JF, Sandberg MN, Birge RR, Knox BE. Conserved residues in the extracellular loops of short-wavelength cone visual pigments. Biochemistry. 2011; 50:6763–6773. [PubMed: 21688771]

Chinen A, Hamaoka T, Yamada Y, Kawamura S. Gene duplication and spectral diversification of cone visual pigments of zebrafish. Genetics. 2003; 163:663–675. [PubMed: 12618404]

Cideciyan AV, Hufnagel RB, Carroll J, Sumaroka A, Luo X, Schwartz SB, Dubra A, Land M, Michaelides M, Gardner JC, Hardcastle AJ, Moore AT, Sisk RA, Ahmed ZM, Kohl S, Wissinger B, Jacobson SG. Human cone visual pigment deletions spare sufficient photoreceptors to warrant gene therapy. Hum. Gene Ther. 2013; 24:993–1006. [PubMed: 24067079]

Collin SP, Trezise AE. The origins of colour vision in vertebrates. Clin. Exp. Optometry. 2004; 87:217–223.

Collin SP, Knight MA, Davies WL, Potter IC, Hunt DM, Trezise AEO. Ancient colour vision: multiple opsin genes in the ancestral vertebrates. Curr. Biol. 2003; 13:R864–R865. [PubMed: 14614838]

Conway BR, Chatterjee S, Field GD, Horwitz GD, Johnson EN, Koida K, Mancuso K. Advances in color science: from retina to behavior. J. Neurosci. 2010; 30:14955–14963. [PubMed: 21068298]

Cooper A. Energy uptake in the first step of visual excitation. Nature. 1979; 282:531–533. [PubMed: 503236]

Coto PB, Sinicropi A, De Vico L, Ferre N, Olivucci M. Characterization of the conical intersection of the visual pigment rhodopsin at the CASPT2//CASSCF/AMBER level of theory. Mol. Phys. 2006a; 104:983–991.

Coto PB, Strambi A, Ferre N, Olivucci M. The color of rhodopsins at the ab initio multiconfigurational perturbation theory resolution. Proc. Natl. Acad. Sci. U. S. A. 2006b; 103:17154–17159. [PubMed: 17090682]

Crognale MA, Teller DY, Motulsky AG, Deeb SS. Severity of color vision defects: electroretinographic (ERG), molecular and behavioral studies. Vis. Res. 1998; 38:3377–3385. [PubMed: 9893852]

Crognale MA, Fry M, Highsmith J, Haegerstrom-Portnoy G, Neitz M, Neitz J, Webster MA. Characterization of a novel form of X-linked incomplete achromatopsia. Vis. Neurosci. 2004; 21:197–203. [PubMed: 15518189]

Curcio CA, Sloan KR, Packer O, Hendrickson AE, Kalina RE. Distribution of cones in human and Monkey retina – individual variability and radial asymmetry. Science. 1987; 236:579–582. [PubMed: 3576186]

Dacey DM. Circuitry for color coding in the primate retina. Proc. Natl. Acad. Sci. U. S. A. 1996; 93:582–588. [PubMed: 8570599]

Dacey DM, Lee BB, Stafford DK, Pokorny J, Smith VC. Horizontal cells of the primate retina: cone specificity without spectral opponency. Science. 1996; 271:656–659. [PubMed: 8571130]

Dalkara D, Duebel J, Sahel JA. Gene therapy for the eye focus on mutation-independent approaches. Curr. Opin. Neurol. 2015; 28:51–60. [PubMed: 25545056]

Dartnall HJ, Bowmaker JK, Mollon JD. Human visual pigments: microspectrophotometric results from the eyes of seven persons. Proc. R. Soc. Lond. B Biol. Sci. 1983; 220:115–130. [PubMed: 6140680]

de Lima EM, Pessoa DM, Sena L, de Melo AG, de Castro PH, Oliveira-Mendes AC, Schneider MP, Pessoa VF. Polymorphic color vision in captive Uta Hick's cuxius, or bearded sakis (Chiropotes utahickae). Am. J. Primatol. 2015; 77:66–75. [PubMed: 25224123]

De Valois RL, De Valois KK. A multi-stage color model. Vis. Res. 1993; 33:1053–1065. [PubMed: 8506645]

De Valois RL, Abramov I, Jacobs GH. Analysis of response patterns of LGN cells. J. Opt. Soc. Am. 1966; 56:966–977. [PubMed: 4959282]

Deeb SS. Molecular genetics of color-vision deficiencies. Vis. Neurosci. 2004; 21:191–196. [PubMed: 15518188]

Deeb SS. The molecular basis of variation in human color vision. Clin. Genet. 2005; 67:369–377. [PubMed: 15811001]

Deeb SS, Lindsey DT, Hibiya Y, Sanocki E, Winderickx J, Teller DY, Motulsky AG. Genotype-phenotype relationships in human red/green color-vision defects: molecular and psychophysical studies. Am. J. Hum. Genet. 1992; 51:687–700. [PubMed: 1415215]

Dilger J, Musbat L, Sheves M, Bochenkova AV, Clemmer DE, Toker Y. Direct measurement of the isomerization barrier of the isolated retinal chromophore. Angew. Chem. Int. Ed. Engl. 2015a; 54:4748–4752. [PubMed: 25756226]

Dilger J, Musbat L, Sheves M, Bochenkova AV, Clemmer DE, Toker Y. Frontispiece: direct measurement of the isomerization barrier of the isolated retinal chromophore. Angew. Chem. Int. Ed. Engl. 2015b; 54

Dillon J, Zheng L, Merriam JC, Gaillard ER. The optical properties of the anterior segment of the eye: implications for cortical cataract. Exp. Eye Res. 1999; 68:785–795. [PubMed: 10375442]

Dominy NJ, Lucas PW. Ecological importance of trichromatic vision to primates. Nature. 2001; 410:363–366. [PubMed: 11268211]

Dryja TP, McGee TL, Reichel E, Hahn LB, Cowley GS, Yandell DW, Sandberg MA, Berson EL. A point mutation of the rhodopsin gene in one form of retinitis pigmentosa. Nature. 1990; 343:364–366. [PubMed: 2137202]

Dunn FA, Lankheet MJ, Rieke F. Light adaptation in cone vision involves switching between receptor and post-receptor sites. Nature. 2007; 449:603–606. [PubMed: 17851533]

Eisner A, Fleming SA, Klein ML, Mauldin WM. Sensitivities in older eyes with good acuity: cross-sectional norms. Invest. Ophthalmol. Vis. Sci. 1987; 28:1824–1831. [PubMed: 3667153]

Farkas MH, Grant GR, White JA, Sousa ME, Consugar MB, Pierce EA. Transcriptome analyses of the human retina identify unprecedented transcript diversity and 3.5 Mb of novel transcribed sequence via significant alternative splicing and novel genes. BMC Genomics. 2013; 14:486. [PubMed: 23865674]

Fischer L, Vorobyev M, Zvyagin A, Plakhotnik T. The Role of an Oil Droplet Lens in Vision Enhancement. Proceedings of the Australian Physiological Society. 1984

Franze K, Grosche J, Skatchkov SN, Schinkinger S, Foja C, Schild D, Uckermann O, Travis K, Reichenbach A, Guck J. Muller cells are living optical fibers in the vertebrate retina. Proc. Natl. Acad. Sci. U. S. A. 2007; 104:8287–8292. [PubMed: 17485670]

Frutos LM, Andruniow T, Santoro F, Ferre N, Olivucci M. Tracking the excited-state time evolution of the visual pigment with multiconfigurational quantum chemistry. Proc. Natl. Acad. Sci. U. S. A. 2007; 104:7764–7769. [PubMed: 17470789]

Fu Y, Kefalov V, Luo DG, Xue T, Yau KW. Quantal noise from human red cone pigment. Nat. Neurosci. 2008; 11:565–571. [PubMed: 18425122]

Fujimoto K, Hasegawa J-y, Hayashi S, Kato S, Nakatsuji H. Mechanism of color tuning in retinal protein: SAC-CI and QM/MM study. Chem. Phys. Lett. 2005; 414:239–242.

Fujimoto K, Hasegawa JY, Hayashi S, Nakatsuji H. On the color-tuning mechanism of human-blue visual pigment: SAC-CI and QM/MM study. Chem. Phys. Lett. 2006; 432:252–256.

Fujimoto K, Hasegawa J, Nakatsuji H. Color tuning mechanism of human red, green, and blue cone pigments: SAC-CI theoretical study. Bull. Chem. Soc. Jpn. 2009; 82:1140–1148.

Garavito RM, Ferguson-Miller S. Detergents as tools in membrane biochemistry. J. Biol. Chem. 2001; 276:32403–32406. [PubMed: 11432878]

Gardner JC, Michaelides M, Holder GE, Kanuga N, Webb TR, Mollon JD, Moore AT, Hardcastle AJ. Blue cone monochromacy: causative mutations and associated phenotypes. Mol. Vis. 2009; 15:876–884. [PubMed: 19421413]

Gardner JC, Webb TR, Kanuga N, Robson AG, Holder GE, Stockman A, Ripamonti C, Ebenezer ND, Ogun O, Devery S, Wright GA, Maher ER, Cheetham ME, Moore AT, Michaelides M, Hardcastle AJ. X-linked cone dystrophy caused by mutation of the red and green cone opsins. Am. J. Hum. Genet. 2010; 87:26–39. [PubMed: 20579627]

Gardner JC, Liew G, Quan YH, Ermetal B, Ueyama H, Davidson AE, Schwarz N, Kanuga N, Chana R, Maher ER, Webster AR, Holder GE, Robson AG, Cheetham ME, Liebelt J, Ruddle JB, Moore AT, Michaelides M, Hardcastle AJ. Three different cone opsin gene array mutational mechanisms with genotype-phenotype correlation and functional investigation of cone opsin variants. Hum. Mutat. 2014; 35:1354–1362. [PubMed: 25168334]

Gegenfurtner KR, Rieger J. Sensory and cognitive contributions of color to the recognition of natural scenes. Curr. Biol. 2000; 10:805–808. [PubMed: 10898985]

Goldsmith TH, Collins JS, Licht S. The cone oil droplets of avian retinas. Vis. Res. 1984; 24:1661–1671. [PubMed: 6533991]

Gozem S, Schapiro I, Ferre N, Olivucci M. The molecular mechanism of thermal noise in rod photoreceptors. Science. 2012; 337:1225–1228. [PubMed: 22955833]

Grau T, Artemyev NO, Rosenberg T, Dollfus H, Haugen OH, Cumhur Sener E, Jurklies B, Andreasson S, Kernstock C, Larsen M, Zrenner E, Wissinger B, Kohl S. Decreased catalytic activity and altered activation properties of PDE6C mutants associated with autosomal recessive achromatopsia. Hum. Mol. Genet. 2011; 20:719–730. [PubMed: 21127010]

Griebel, U. Color vision in marine mammals: a review. In: Bright, M.; Dworschak, PC.; Stachowitsch, M., editors. The Vienna School of Marine Biology: a Tribute to Jöorg Ott. Wien: Facultas Universitätsverlag; 2002. p. 73-87.

Griffin DR, Hubbard R, Wald G. The sensitivity of the human eye to infrared radiation. J. Opt. Soc. Am. 1947; 37:546–554. [PubMed: 20256359]

Gunther KL, Neitz J, Neitz M. A novel mutation in the short-wavelength-sensitive cone pigment gene associated with a tritan color vision defect. Vis. Neurosci. 2006; 23:403–409. [PubMed: 16961973]

Guo Y, Sekharan S, Liu J, Batista VS, Tully JC, Yan EC. Unusual kinetics of thermal decay of dim-light photoreceptors in vertebrate vision. Proc. Natl. Acad. Sci. U. S. A. 2014; 111:10438–10443. [PubMed: 25002518]

Gupta P, Guo H, Atchison DA, Zele AJ. Effect of optical aberrations on the color appearance of small defocused lights. J. Opt. Soc. Am. A Opt. Image Sci. Vis. 2010; 27:960–967. [PubMed: 20448760]

Hammond BR Jr, Wooten BR, Snodderly DM. Individual variations in the spatial profile of human macular pigment. J. Opt. Soc. Am. A Opt. Image Sci. Vis. 1997; 14:1187–1196. [PubMed: 9168592]

Hannover, A. Über die Netzhaut und ihre Gehinsubstanz bei Wirbelthieren, mit Ausnahme des Menschen. In: Müller, J., editor. Arch. Anat. Physiol. Wiss. Med. 1840. p. 320-345.

Hansen T, Pracejus L, Gegenfurtner KR. Color perception in the intermediate periphery of the visual field. J. Vis. 2009; 9(26):1–12.

Hart NS, Lisney TJ, Collin SP. Cone photoreceptor oil droplet pigmentation is affected by ambient light intensity. J. Exp. Biol. 2006; 209:4776–4787. [PubMed: 17114410]

Hayashi T, Kubo A, Takeuchi T, Gekka T, Goto-Omoto S, Kitahara K. Novel form of a single X-linked visual pigment gene in a unique dichromatic color-vision defect. Vis. Neurosci. 2006; 23:411–417. [PubMed: 16961974]

Hirano T, Imai H, Kandori H, Shichida Y. Chloride effect on iodopsin studied by low-temperature visible and infrared spectroscopies. Biochemistry. 2001; 40:1385–1392. [PubMed: 11170466]

Hirsch J, Fau - Miller WH, Miller WH. Does cone positional disorder limit resolution? J. Opt. Soc. Am. A. 1987; 4:1481–1492. [PubMed: 3625328]

Hofer H, Carroll J, Neitz J, Neitz M, Williams DR. Organization of the human trichromatic cone mosaic. J. Neurosci. 2005; 25:9669–9679. [PubMed: 16237171]

Horiguchi H, Winawer J, Dougherty RF, Wandell BA. Human trichromacy revisited. Proc. Natl. Acad. Sci. U. S. A. 2013; 110:E260–E269. [PubMed: 23256158]

Horton JC, Hoyt WF. The representation of the visual field in human striate cortex. A revision of the classic Holmes map. Arch. Ophthalmol. 1991; 109:816–824. [PubMed: 2043069]

Hunt DM, Peichl L. S cones: evolution, retinal distribution, development, and spectral sensitivity. Vis. Neurosci. 2014; 31:115–138. [PubMed: 23895771]

Hunt DM, Carvalho LS, Cowing JA, Davies WL. Evolution and spectral tuning of visual pigments in birds and mammals. Philos. Trans. R. Soc. Lond. B Biol. Sci. 2009; 364:2941–2955. [PubMed: 19720655]

Huntress MM, Gozem S, Malley KR, Jailaubekov AE, Vasileiou C, Vengris M, Geiger JH, Borhan B, Schapiro I, Larsen DS, Olivucci M. Toward an understanding of the retinal chromophore in rhodopsin mimics. J. Phys. Chem. B. 2013; 117:10053–10070. [PubMed: 23971945]

Imai H, Kuwayama S, Onishi A, Morizumi T, Chisaka O, Shichida Y. Molecular properties of rod and cone visual pigments from purified chicken cone pigments to mouse rhodopsin in situ. Photochem Photobiol. Sci. 2005; 4:667–674. [PubMed: 16121275]

Imamoto Y, Shichida Y. Cone visual pigments. Biochim. Biophys. Acta. 2014; 1837:664–673. [PubMed: 24021171]

Ives JT, Normann RA, Barber PW. Light intensification by cone oil droplets: electromagnetic considerations. J. Opt. Soc. Am. 1983; 73:1725–1731.

Jacobs GH. The distribution and nature of colour vision among the mammals. Biol. Rev. Camb. Philos. Soc. 1993; 68:413–471. [PubMed: 8347768]

Jacobs GH. Primate color vision: a comparative perspective. Vis. Neurosci. 2008; 25:619–633. [PubMed: 18983718]

Jacobs GH. Evolution of colour vision in mammals. Philos. Trans. R. Soc. Lond. B Biol. Sci. 2009; 364:2957–2967. [PubMed: 19720656]

Jacobs GH, Nathans J. The evolution of primate color vision. Sci. Am. 2009; 300:56–63. [PubMed: 19363921]

Jacobs GH, Williams GA, Fenwick JA. Influence of cone pigment coexpression on spectral sensitivity and color vision in the mouse. Vis. Res. 2004; 44:1615–1622. [PubMed: 15135998]

Jagla WM, Jagle H, Hayashi T, Sharpe LT, Deeb SS. The molecular basis of dichromatic color vision in males with multiple red and green visual pigment genes. Hum. Mol. Genet. 2002; 11:23–32. [PubMed: 11772996]

Johnson CA, Adams AJ, Twelker JD, Quigg JM. Age-related changes in the central visual field for short-wavelength-sensitive pathways. J. Opt. Soc. Am. A. 1988; 5:2131–2139. [PubMed: 3230482]

Jordan G, Deeb SS, Bosten JM, Mollon JD. The dimensionality of color vision in carriers of anomalous trichromacy. J. Vis. 2010; 10:12. [PubMed: 20884587]

Karl, R.; Gegenfurtner, LTS. Color Vision: from Genes to Perception. Cambridge University Press; 2001.

Kawamura S, Yokoyama S. Molecular characterization of the red visual pigment gene of the American chameleon (Anolis-Carolinensis). Febs Lett. 1993; 323:247–251. [PubMed: 8500618]

Kefalov VJ. Rod and cone visual pigments and phototransduction through pharmacological, genetic, and physiological approaches. J. Biol. Chem. 2012; 287:1635–1641. [PubMed: 22074928]

Kefalov V, Fu Y, Marsh-Armstrong N, Yau KW. Role of visual pigment properties in rod and cone phototransduction. Nature. 2003; 425:526–531. [PubMed: 14523449]

Kefalov VJ, Estevez ME, Kono M, Goletz PW, Crouch RK, Cornwall MC, Yau KW. Breaking the covalent bond–a pigment property that contributes to desensitization in cones. Neuron. 2005; 46:879–890. [PubMed: 15953417]

Kessel L, Lundeman JH, Herbst K, Andersen TV, Larsen M. Age-related changes in the transmission properties of the human lens and their relevance to circadian entrainment. J. Cataract. Refract Surg. 2010; 36:308–312. [PubMed: 20152615]

Kim JE, Tauber MJ, Mathies RA. Wavelength dependent cis-trans isomerization in vision. Biochemistry. 2001; 40:13774–13778. [PubMed: 11705366]

Kim JE, Tauber MJ, Mathies RA. Analysis of the mode-specific excited-state energy distribution and wavelength-dependent photoreaction quantum yield in rhodopsin. Biophys. J. 2003; 84:2492–2501. [PubMed: 12668457]

Kirschfeld K, Franceschini N, Minke B. Evidence for a sensitising pigment in fly photoreceptors. Nature. 1977; 269:386–390. [PubMed: 909585]

Kiser PD, Golczak M, Palczewski K. Chemistry of the retinoid (visual) cycle. Chem. Rev. 2014; 114:194–232. [PubMed: 23905688]

Knott B, Berg ML, Morgan ER, Buchanan KL, Bowmaker JK, Bennett AT. Avian retinal oil droplets: dietary manipulation of colour vision? Proc. Biol. Sci. 2010; 277:953–962. [PubMed: 19939843]

Koenig D, Hofer H. The absolute threshold of cone vision. J. Vis. 2011; 11

Kohl S, Marx T, Giddings I, Jagle H, Jacobson SG, Apfelstedt-Sylla E, Zrenner E, Sharpe LT, Wissinger B. Total colourblindness is caused by mutations in the gene encoding the alpha-subunit of the cone photoreceptor cGMP-gated cation channel. Nat. Genet. 1998; 19:257–259. [PubMed: 9662398]

Kohl S, Baumann B, Broghammer M, Jagle H, Sieving P, Kellner U, Spegal R, Anastasi M, Zrenner E, Sharpe LT, Wissinger B. Mutations in the CNGB3 gene encoding the beta-subunit of the cone photoreceptor cGMP-gated channel are responsible for achromatopsia (ACHM3) linked to chromosome 8q21. Hum. Mol. Genet. 2000; 9:2107–2116. [PubMed: 10958649]

Kohl S, Baumann B, Rosenberg T, Kellner U, Lorenz B, Vadala M, Jacobson SG, Wissinger B. Mutations in the cone photoreceptor G-protein alpha-subunit gene GNAT2 in patients with achromatopsia. Am. J. Hum. Genet. 2002; 71:422–425. [PubMed: 12077706]

Kolb, H. The Organization of the Retina and Visual System FED. Helga: Kolb; 2015. Facts and Figures Concerning the Human Retina BTI - Webvision.

Korenbrot JI. Speed, sensitivity, and stability of the light response in rod and cone photoreceptors: facts and models. Prog. Retin. Eye Res. 2012; 31:442–466. [PubMed: 22658984]

Koskelainen A, Ala-Laurila P, Fyhrquist N, Donner K. Measurement of thermal contribution to photoreceptor sensitivity. Nature. 2000; 403:220–223. [PubMed: 10646610]

Krill AE, Smith VC, Pokorny J. Further studies supporting the identity of congenital tritanopia and hereditary dominant optic atrophy. Invest. Ophthalmol. Vis. Sci. 1971; 10:457–465.

Kuemmel CM, Sandberg MN, Birge RR, Knox BE. A conserved aromatic residue regulating photosensitivity in short-wavelength sensitive cone visual pigments. Biochemistry. 2013; 52:5084–5091. [PubMed: 23808485]

Labin AM, Safuri SK, Ribak EN, Perlman I. Muller cells separate between wavelengths to improve day vision with minimal effect upon night vision. Nat. Commun. 2014; 5:4319. [PubMed: 25003477]

Lamb TD. Evolution of phototransduction, vertebrate photoreceptors and retina. Prog. Retin Eye Res. 2013; 36:52–119. [PubMed: 23792002]

Land MF, Osorio D. Extraordinary color vision. Science. 2014; 343:381–382. [PubMed: 24458632]

Lee BB. Color coding in the primate visual pathway: a historical view. J. Opt. Soc. Am. A Opt. Image Sci. Vis. 2014; 31:A103–A112. [PubMed: 24695157]

Lei B, Yao G. Spectral attenuation of the mouse, rat, pig and human lenses from wavelengths 360 nm to 1020 nm. Exp. Eye Res. 2006; 83:610–614. [PubMed: 16682025]

Lewis PR. A theoretical interpretation of spectral sensitivity curves at long wavelengths. J. Physiol. 1955; 130:45–52. [PubMed: 13278884]

Lewis JW, Szundi I, Fu WY, Sakmar TP, Kliger DS. pH dependence of photolysis intermediates in the photoactivation of rhodopsin mutant E113Q. Biochemistry. 2000; 39:599–606. [PubMed: 10642185]

Liu RS, Colmenares LU. The molecular basis for the high photosensitivity of rhodopsin. Proc. Natl. Acad. Sci. U. S. A. 2003; 100:14639–14644. [PubMed: 14657350]

Liu J, Liu MY, Nguyen JB, Bhagat A, Mooney V, Yan EC. Thermal decay of rhodopsin: role of hydrogen bonds in thermal isomerization of 11-cis retinal in the binding site and hydrolysis of protonated Schiff base. J. Am. Chem. Soc. 2009; 131:8750–8751. [PubMed: 19505100]

Liu J, Liu MY, Fu L, Zhu GA, Yan EC. Chemical kinetic analysis of thermal decay of rhodopsin reveals unusual energetics of thermal isomerization and hydrolysis of Schiff base. J. Biol. Chem. 2011; 286:38408–38416. [PubMed: 21921035]

Lombardo M, Serrao S, Ducoli P, Lombardo G. Eccentricity dependent changes of density, spacing and packing arrangement of parafoveal cones. Ophthalmic Physiol. Opt. 2013a; 33:516–526. [PubMed: 23550537]

Lombardo M, Serrao S, Ducoli P, Lombardo G. Influence of sampling window size and orientation on parafoveal cone packing density. Biomed. Opt. Express. 2013b; 4:1318–1331. [PubMed: 24009995]

Lorenz-Fonfria VA, Furutani Y, Ota T, Ido K, Kandori H. Protein fluctuations as the possible origin of the thermal activation of rod photoreceptors in the dark. J. Am. Chem. Soc. 2010; 132:5693–5703. [PubMed: 20356096]

Lukats A, Szabo A, Rohlich P, Vigh B, Szel A. Photopigment coexpression in mammals: comparative and developmental aspects. Histol. Histopathol. 2005; 20:551–574. [PubMed: 15736061]

Luo Y-R. Why is the human visual system sensitive only to light of wavelengths from approximately 760 to 380 nm?: an answer from thermochemistry and chemical kinetics. Biophys. Chem. 2000; 83:179–184. [PubMed: 10647848]

Luo DG, Xue T, Yau KW. How vision begins: an odyssey. Proc. Natl. Acad. Sci. U. S. A. 2008; 105:9855–9862. [PubMed: 18632568]

Luo DG, Yue WW, Ala-Laurila P, Yau KW. Activation of visual pigments by light and heat. Science. 2011; 332:1307–1312. [PubMed: 21659602]

Lythgoe RJ, Quilliam JP. The thermal decomposition of visual purple. J. Physiol. 1938; 93:24–38. [PubMed: 16994991]

Mancuso K, Hauswirth WW, Li Q, Connor TB, Kuchenbecker JA, Mauck MC, Neitz J, Neitz M. Gene therapy for red-green colour blindness in adult primates. Nature. 2009; 461:784–787. [PubMed: 19759534]

Mancuso K, Mauck MC, Kuchenbecker JA, Neitz M, Neitz J. A multi-stage color model revisited: implications for a gene therapy cure for red-green colorblindness. Adv. Exp. Med. Biol. 2010; 664:631–638. [PubMed: 20238067]

Marshall J, Oberwinkler J. The colourful world of the mantis shrimp. Nature. 1999; 401:873–874. [PubMed: 10553902]

Martinez-Mayorga K, Pitman MC, Grossfield A, Feller SE, Brown MF. Retinal counterion switch mechanism in vision evaluated by molecular simulations. J. Am. Chem. Soc. 2006; 128:16502–16503. [PubMed: 17177390]

Masuda T, Zhang X, Berlinicke C, Wan J, Yerrabelli A, Conner EA, Kjellstrom S, Bush R, Thorgeirsson SS, Swaroop A, Chen S, Zack DJ. The transcription factor GTF2IRD1 regulates the

topology and function of photoreceptors by modulating photoreceptor gene expression across the retina. J. Neurosci. 2014; 34:15356–15368. [PubMed: 25392503]

Matsui S, Seidou M, Uchiyama I, Sekiya N, Hiraki K, Yoshihara K, Kito Y. 4-Hydroxyretinal, a new visual pigment chromophore found in the bioluminescent squid, Watasenia-Scintillans. Biochim. Biophys. Acta. 1988; 966:370–374. [PubMed: 3416013]

Matsumoto Y, Hiramatsu C, Matsushita Y, Ozawa N, Ashino R, Nakata M, Kasagi S, Di Fiore A, Schaffner CM, Aureli F, Melin AD, Kawamura S. Evolutionary renovation of L/M opsin polymorphism confers a fruit discrimination advantage to ateline new world monkeys. Mol. Ecol. 2014; 23:1799–1812. [PubMed: 24612406]

McBee JK, Van Hooser JP, Jang GF, Palczewski K. Isomerization of 11-cis-retinoids to all-trans-retinoids in vitro and in vivo. J. Biol. Chem. 2001; 276:48483–48493. [PubMed: 11604395]

McClements M, Davies WI, Michaelides M, Carroll J, Rha J, Mollon JD, Neitz M, MacLaren RE, Moore AT, Hunt DM. X-linked cone dystrophy and colour vision deficiency arising from a missense mutation in a hybrid L/M cone opsin gene. Vis. Res. 2013; 80:41–50. [PubMed: 23337435]

McMahon C, Carroll J, Awua S, Neitz J, Neitz M. The L: M cone ratio in males of African descent with normal color vision. J. Vis. 2008; 8(5):1–9. [PubMed: 18318631]

Melaccio F, Ferre N, Olivucci M. Quantum chemical modeling of rhodopsin mutants displaying switchable colors. Phys. Chem. Chem. Phys. 2012; 14:12485–12495. [PubMed: 22699180]

Melin AD, Danosi CF, McCracken GF, Dominy NJ. Dichromatic vision in a fruit bat with diurnal proclivities: the Samoan flying fox (Pteropus samoensis). J. Comp. Physiol. A Neuroethol. Sens. Neural Behav. Physiol. 2014; 200:1015–1022. [PubMed: 25319538]

Merbs SL, Nathans J. Absorption spectra of human cone pigments. Nature. 1992; 356:433–435. [PubMed: 1557124]

Mizrahi-Meissonnier L, Merin S, Banin E, Sharon D. Variable retinal phenotypes caused by mutations in the X-linked photopigment gene array. Invest. Ophthalmol. Vis. Sci. 2010; 51:3884–3892. [PubMed: 20220053]

Mollon JD, Regan BC, Bowmaker JK. What is the function of the cone-rich rim of the retina? Eye. 1998; 12:548–552. [PubMed: 9775216]

Mooney V, Sekharan S, Liu J, Guo Y, Batista VS, Yan EC. Kinetics of thermal activation of an ultraviolet cone pigment. J. Am. Chem. Soc. 2015; 137:307–313. [PubMed: 25514632]

Morizumi T, Sato K, Shichida Y. Spectroscopic analysis of the effect of chloride on the active intermediates of the primate L group cone visual pigment. Biochemistry. 2012; 51:10017–10023. [PubMed: 23176664]

Müller GE. Über die Farbenempfindungen. Z. Psychol. Physiol. Sinnesorgane Erganzungsbände 17 and 18. 1930; (1–430):435–647.

Mustafi D, Engel AH, Palczewski K. Structure of cone photoreceptors. Prog. Retin Eye Res. 2009; 28:289–302. [PubMed: 19501669]

Nathans J. Determinants of visual pigment absorbance – role of charged amino-acids in the putative transmembrane segments. Biochemistry. 1990; 29:937–942. [PubMed: 2111169]

Nathans J. The evolution and physiology of human color vision: insights from molecular genetic studies of visual pigments. Neuron. 1999; 24:299–312. [PubMed: 10571225]

Nathans J, Piantanida TP, Eddy RL, Shows TB, Hogness DS. Molecular genetics of inherited variation in human color vision. Science. 1986a; 232:203–210. [PubMed: 3485310]

Nathans J, Thomas D, Hogness DS. Molecular genetics of human color vision: the genes encoding blue, green, and red pigments. Science. 1986b; 232:193–202. [PubMed: 2937147]

Nathans J, Davenport CM, Maumenee IH, Lewis RA, Hejtmancik JF, Litt M, Lovrien E, Weleber R, Bachynski B, Zwas F, et al. Molecular genetics of human blue cone monochromacy. Science. 1989; 245:831–838. [PubMed: 2788922]

Nathans J, Maumenee IH, Zrenner E, Sadowski B, Sharpe LT, Lewis RA, Hansen E, Rosenberg T, Schwartz M, Heckenlively JR, et al. Genetic heterogeneity among blue-cone monochromats. Am. J. Hum. Genet. 1993; 53:987–1000. [PubMed: 8213841]

Neitz J, Jacobs GH. Polymorphism of the long-wavelength cone in normal human colour vision. Nature. 1986; 323:623–625. [PubMed: 3773989]

Neitz M, Neitz J. Numbers and ratios of visual pigment genes for normal red-green color vision. Science. 1995; 267:1013–1016. [PubMed: 7863325]

Neitz J, Neitz M. The genetics of normal and defective color vision. Vis. Res. 2011; 51:633–651. [PubMed: 21167193]

Neitz J, Neitz M, Jacobs GH. Analysis of fusion gene and encoded photopigment of colour-blind humans. Nature. 1989; 342:679–682. [PubMed: 2574415]

Neitz J, Neitz M, Kainz PM. Visual pigment gene structure and the severity of color vision defects. Science. 1996; 274:801–804. [PubMed: 8864125]

Neitz M, Carroll J, Renner A, Knau H, Werner JS, Neitz J. Variety of genotypes in males diagnosed as dichromatic on a conventional clinical anomaloscope. Vis. Neurosci. 2004; 21:205–216. [PubMed: 15518190]

Norren DV, Vos JJ. Spectral transmission of the human ocular media. Vis. Res. 1974; 14:1237–1244. [PubMed: 4428632]

Ohlendorf A, Tabernero J, Schaeffel F. Visual acuity with simulated and real astigmatic defocus. Optom. Vis. Sci. 2011; 88:562–569. [PubMed: 21460757]

Okada T, Fujiyoshi Y, Silow M, Navarro J, Landau EM, Shichida Y. Functional role of internal water molecules in rhodopsin revealed by X-ray crystallography. Proc. Natl. Acad. Sci. U. S. A. 2002; 99:5982–5987. [PubMed: 11972040]

Okano T, Kojima D, Fukada Y, Shichida Y, Yoshizawa T. Primary structures of chicken cone visual pigments: vertebrate rhodopsins have evolved out of cone visual pigments. Proc. Natl. Acad. Sci. U. S. A. 1992; 89:5932–5936. [PubMed: 1385866]

Oprian DD, Asenjo AB, Lee N, Pelletier SL. Design, chemical synthesis, and expression of genes for the three human color vision pigments. Biochemistry. 1991; 30:11367–11372. [PubMed: 1742276]

Orban T, Jastrzebska B, Palczewski K. Structural approaches to understanding retinal proteins needed for vision. Curr. Opin. Cell Biol. 2014; 27:32–43. [PubMed: 24680428]

Pahlberg J, Sampath AP. Visual threshold is set by linear and nonlinear mechanisms in the retina that mitigate noise. BioEssays. 2011; 33:438–447. [PubMed: 21472740]

Palczewska G, Vinberg F, Stremplewski P, Bircher MP, Salom D, Komar K, Zhang J, Cascella M, Wojtkowski M, Kefalov VJ, Palczewski K. Human infrared vision is triggered by two-photon chromophore isomerization. Proc. Natl. Acad. Sci. U. S. A. 2014; 111:E5445–E5454. [PubMed: 25453064]

Palczewski K. G protein-coupled receptor rhodopsin. Annu. Rev. Biochem. 2006; 75:743–767. [PubMed: 16756510]

Palczewski K. Chemistry and biology of vision. J. Biol. Chem. 2012; 287:1612–1619. [PubMed: 22074921]

Palczewski K, Kumasaka T, Hori T, Behnke CA, Motoshima H, Fox BA, Le Trong I, Teller DC, Okada T, Stenkamp RE, Yamamoto M, Miyano M. Crystal structure of rhodopsin: a G protein-coupled receptor. Science. 2000; 289:739–745. [PubMed: 10926528]

Paleologos EK, Giokas DL, Karayannis MI. Micelle-mediated separation and cloud-point extraction. TrAC Trends Anal. Chem. 2005; 24:426–436.

Peichl L. Diversity of mammalian photoreceptor properties: adaptations to habitat and lifestyle? Anat. Rec. A Discov. Mol. Cell Evol. Biol. 2005; 287:1001–1012. [PubMed: 16200646]

Peichl L, Behrmann G, Kröger RHH. For whales and seals the ocean is not blue: a visual pigment loss in marine mammals*. Eur. J. Neurosci. 2001; 13:1520–1528. [PubMed: 11328346]

Peng GH, Chen S. Active opsin loci adopt intrachromosomal loops that depend on the photoreceptor transcription factor network. Proc. Natl. Acad. Sci. U. S. A. 2011; 108:17821–17826. [PubMed: 22006320]

Pokorny J, Smith VC, Went LN. Color matching in autosomal dominant tritan defect. J. Opt. Soc. Am. 1981; 71:1327–1334. [PubMed: 6977627]

Polans A, Baehr W, Palczewski K. Turned on by Ca2+! the physiology and pathology of Ca(2+)-binding proteins in the retina. Trends Neurosci. 1996; 19:547–554. [PubMed: 8961484]

Polli D, Altoe P, Weingart O, Spillane KM, Manzoni C, Brida D, Tomasello G, Orlandi G, Kukura P, Mathies RA, Garavelli M, Cerullo G. Conical intersection dynamics of the primary photoisomerization event in vision. Nature. 2010; 467:440–443. [PubMed: 20864998]

Provis JM, Dubis AM, Maddess T, Carroll J. Adaptation of the central retina for high acuity vision: cones, the fovea and the avascular zone. Prog. Retin Eye Res. 2013; 35:63–81. [PubMed: 23500068]

Pum D, Ahnelt PK, Grasl M. Iso-orientation areas in the foveal cone mosaic. Vis. Neurosci. 1990; 5:511–523. [PubMed: 2085468]

Rajamani R, Lin YL, Gao J. The opsin shift and mechanism of spectral tuning in rhodopsin. J. Comput. Chem. 2011; 32:854–865. [PubMed: 20941732]

Ramos LS, Chen MH, Knox BE, Birge RR. Regulation of photoactivation in vertebrate short wavelength visual pigments: protonation of the retinylidene Schiff base and a counterion switch. Biochemistry. 2007; 46:5330–5340. [PubMed: 17439245]

Regan BC, Julliot C, Simmen B, Vienot F, Charles-Dominique P, Mollon JD. Fruits, foliage and the evolution of primate colour vision. Philos. Trans. R. Soc. Lond. B Biol. Sci. 2001; 356:229–283. [PubMed: 11316480]

Reitner A, Sharpe LT, Zrenner E. Is colour vision possible with only rods and blue-sensitive cones? Nature. 1991; 352:798–800. [PubMed: 1881435]

Reyniers E, Van Thienen MN, Meire F, De Boulle K, Devries K, Kestelijn P, Willems PJ. Gene conversion between red and defective green opsin gene in blue cone monochromacy. Genomics. 1995; 29:323–328. [PubMed: 8666378]

Ridge KD, Abdulaev NG, Sousa M, Palczewski K. Phototransduction: crystal clear. Trends Biochem. Sci. 2003; 28:479–487. [PubMed: 13678959]

Rieke F, Baylor DA. Single-photon detection by rod cells of the retina. Rev. Mod. Phys. 1998; 70:1027–1036.

Rieke F, Baylor DA. Origin and functional impact of dark noise in retinal cones. Neuron. 2000; 26:181–186. [PubMed: 10798402]

Rinaldi S, Melaccio F, Gozem S, Fanelli F, Olivucci M. Comparison of the isomerization mechanisms of human melanopsin and invertebrate and vertebrate rhodopsins. Proc. Natl. Acad. Sci. U. S. A. 2014; 111:1714–1719. [PubMed: 24449866]

Robinson SR. Early vertebrate colour vision. Nature. 1994; 367:121–121. [PubMed: 8114909]

Rohlich P, van Veen T, Szel A. Two different visual pigments in one retinal cone cell. Neuron. 1994; 13:1159–1166. [PubMed: 7946352]

Roosing S, Thiadens AAHJ, Hoyng CB, Klaver CCW, den Hollander AI, Cremers FPM. Causes and consequences of inherited cone disorders. Prog. Retin. Eye Res. 2014; 42:1–26. [PubMed: 24857951]

Rowe MH. Trichromatic color vision in primates. News Physiol. Sci. 2002; 17:93–98. [PubMed: 12021378]

Rucker FJ, Osorio D. The effects of longitudinal chromatic aberration and a shift in the peak of the middle-wavelength sensitive cone fundamental on cone contrast. Vis. Res. 2008; 48:1929–1939. [PubMed: 18639571]

Rynders M, Lidkea B, Chisholm W, Thibos LN. Statistical distribution of foveal transverse chromatic aberration, pupil centration, and angle psi in a population of young adult eyes. J. Opt. Soc. Am. A Opt. Image Sci. Vis. 1995; 12:2348–2357. [PubMed: 7500216]

Sabesan R, Yoon G. Neural compensation for long-term asymmetric optical blur to improve visual performance in keratoconic eyes. Invest. Ophthalmol. Vis. Sci. 2010; 51:3835–3839. [PubMed: 20130284]

Sakmar TP. Biochemistry. Redder than red. Science. 2012; 338:1299–1300. [PubMed: 23224543]

Salon JA, Lodowski DT, Palczewski K. The significance of G protein-coupled receptor crystallography for drug discovery. Pharmacol. Rev. 2011; 63:901–937. [PubMed: 21969326]

Sandkam B, Young CM, Breden F. Beauty in the eyes of the beholders: colour vision is tuned to mate preference in the Trinidadian guppy (Poecilia reticulata). Mol. Ecol. 2015; 24:596–609. [PubMed: 25556876]

Santos-Ferreira T, Postel K, Stutzki H, Kurth T, Zeck G, Ader M. Daylight vision repair by cell transplantation. Stem Cells. 2015; 33:79–90. [PubMed: 25183393]

Schmidt BP, Neitz M, Neitz J. Neurobiological hypothesis of color appearance and hue perception. J. Opt. Soc. Am. A Opt. Image Sci. Vis. 2014a; 31:A195–A207. [PubMed: 24695170]

Schmidt TM, Alam NM, Chen S, Kofuji P, Li W, Prusky GT, Hattar S. A role for melanopsin in alpha retinal ganglion cells and contrast detection. Neuron. 2014b; 82:781–788. [PubMed: 24853938]

Sekharan S, Katayama K, Kandori H, Morokuma K. Color vision: “OH-site” rule for seeing red and green. J. Am. Chem. Soc. 2012; 134:10706–10712. [PubMed: 22663599]

Sekharan S, Mooney VL, Rivalta I, Kazmi MA, Neitz M, Neitz J, Sakmar TP, Yan EC, Batista VS. Spectral tuning of ultraviolet cone pigments: an interhelical lock mechanism. J. Am. Chem. Soc. 2013; 135:19064–19067. [PubMed: 24295328]

Seki T, Vogt K. Evolutionary aspects of the diversity of visual pigment chromophores in the class insecta. Comp. Biochem. Physiol. B Biochem. Mol. Biol. 1998; 119:53–64.

Seko Y, Azuma N, Ishii T, Komuta Y, Miyamoto K, Miyagawa Y, Kaneda M, Umezawa A. Derivation of human differential photoreceptor cells from adult human dermal fibroblasts by defined combinations of CRX, RAX, OTX2 and NEUROD. Genes Cells. 2014; 19:198–208. [PubMed: 24456169]

Shi G, Yau KW, Chen J, Kefalov VJ. Signaling properties of a short-wave cone visual pigment and its role in phototransduction. J. Neurosci. 2007; 27:10084–10093. [PubMed: 17881515]

Shinomori K, Werner JS. Aging of human short-wave cone pathways. Proc. Natl. Acad. Sci. U. S. A. 2012; 109:13422–13427. [PubMed: 22847416]

Shinomori K, Schefrin BE, Werner JS. Age-related changes in wavelength discrimination. J. Opt. Soc. Am. A Opt. Image Sci. Vis. 2001; 18:310–318. [PubMed: 11205976]

Smith DP, Cole BL, Isaacs A. Congenital tritanopia without neuroretinal disease. Invest. Ophthalmol. 1973; 12:608–617. [PubMed: 4542649]

St George RC. The interplay of light and heat in bleaching rhodopsin. J. Gen. Physiol. 1952; 35:495–517. [PubMed: 14898032]

Stalikas CD. Micelle-mediated extraction as a tool for separation and pre-concentration in metal analysis. TrAC Trends Anal. Chem. 2002; 21:343–355.

Stenkamp RE, Filipek S, Driessen CA, Teller DC, Palczewski K. Crystal structure of rhodopsin: a template for cone visual pigments and other G protein-coupled receptors. Biochim. Biophys. Acta. 2002; 1565:168–182. [PubMed: 12409193]

Stiles, WS. Transactions of the Optical Convention of the Worshipful Company of Spectacle Makers. London: Spectacle Makers' Co; 1948. The Physical Interpretation of the Spectral Sensitivity Curve of the Eye; p. 97-107.

Stockman, A.; Brainard, DH. COLOR VISION MECHANISMS, the Optical Society of America Handbook of Optics: Vision and Vision Optics. New York: McGraw Hill; 2010.

Stockman A, Sharpe LT. The spectral sensitivities of the middle- and long-wavelength-sensitive cones derived from measurements in observers of known genotype. Vis. Res. 2000; 40:1711–1737. [PubMed: 10814758]

Stockman A, MacLeod DI, Johnson NE. Spectral sensitivities of the human cones. J. Opt. Soc. Am. A Opt. Image Sci. Vis. 1993; 10:2491–2521. [PubMed: 8301403]

Sugihara M, Buss V, Entel P, Elstner M, Frauenheim T. 11-cis-retinal protonated Schiff base: influence of the protein environment on the geometry of the rhodopsin chromophore. Biochemistry. 2002; 41:15259–15266. [PubMed: 12484764]

Sui X, Kiser PD, Lintig J, Palczewski K. Structural basis of carotenoid cleavage: from bacteria to mammals. Arch. Biochem. Biophys. 2013; 539:203–213. [PubMed: 23827316]

Sun H, Macke JP, Nathans J. Mechanisms of spectra tuning in the mouse green cone pigment. Proc. Natl. Acad. Sci. U. S. A. 1997; 94:8860–8865. [PubMed: 9238068]

Suzuki T, Makinotasaka M, Eguchi E. 3-Dehydroretinal (Vitamin-a-2 aldehyde) in crayfish eye. Vis. Res. 1984a; 24:783–787. [PubMed: 6474835]

Suzuki T, Makinotasaka M, Miyata S. Competition between retinal and 3-Dehydroretinal for opsin in the regeneration of visual pigment. Zoological Sci. 1984b; 1:861–861.

Szel A, Csorba G, Caffe AR, Szel G, Rohlich P, Vanveen T. Different patterns of retinal cone topography in 2 Genera of rodents, Mus and Apodemus. Cell Tissue Res. 1994a; 276:143–150. [PubMed: 8187156]

Szel A, van Veen T, Rohlich P. Retinal cone differentiation. Nature. 1994b; 370:336. [PubMed: 8047139]

Szel A, Lukats A, Fekete T, Szepessy Z, Rohlich P. Photoreceptor distribution in the retinas of subprimate mammals. J. Opt. Soc. Am. A Opt. Image Sci. Vis. 2000; 17:568–579. [PubMed: 10708038]

Szikra T, Trenholm S, Drinnenberg A, Juttner J, Raics Z, Farrow K, Biel M, Awatramani G, Clark DA, Sahel JA, da Silveira RA, Roska B. Rods in daylight act as relay cells for cone-driven horizontal cell-mediated surround inhibition. Nat. Neurosci. 2014; 17:1728–1735. [PubMed: 25344628]

Teller DC, Stenkamp RE, Palczewski K. Evolutionary analysis of rhodopsin and cone pigments: connecting the three-dimensional structure with spectral tuning and signal transfer. FEBS Lett. 2003; 555:151–159. [PubMed: 14630336]

Terakita A, Yamashita T, Shichida Y. Highly conserved glutamic acid in the extracellular IV-V loop in rhodopsins acts as the counterion in retinochrome, a member of the rhodopsin family. Proc. Natl. Acad. Sci. U. S. A. 2000; 97:14263–14267. [PubMed: 11106382]

Terakita A, Koyanagi M, Tsukamoto H, Yamashita T, Miyata T, Shichida Y. Counterion displacement in the molecular evolution of the rhodopsin family. Nat. Struct. Mol. Biol. 2004; 11:284–289. [PubMed: 14981504]

Thiadens AA, den Hollander AI, Roosing S, Nabuurs SB, Zekveld-Vroon RC, Collin RW, De Baere E, Koenekoop RK, van Schooneveld MJ, Strom TM, van Lith-Verhoeven JJ, Lotery AJ, van Moll-Ramirez N, Leroy BP, van den Born LI, Hoyng CB, Cremers FP, Klaver CC. Homozygosity mapping reveals PDE6C mutations in patients with early-onset cone photoreceptor disorders. Am. J. Hum. Genet. 2009; 85:240–247. [PubMed: 19615668]

Thoen HH, How MJ, Chiou TH, Marshall J. A different form of color vision in Mantis shrimp. Science. 2014; 343:411–413. [PubMed: 24458639]

Tolhurst DJ, Ling L. Magnification factors and the organization of the human striate cortex. Hum. Neurobiol. 1988; 6:247–254. [PubMed: 2832355]

Toyama M, Hironaka M, Yamahama Y, Horiguchi H, Tsukada O, Uto N, Ueno Y, Tokunaga F, Seno K, Hariyama T. Presence of rhodopsin and porphyropsin in the eyes of 164 fishes, representing marine, diadromous, coastal and freshwater species - a qualitative and comparative study. Photochem. Photobiol. 2008; 84:996–1002. [PubMed: 18422881]

Ueyama H, Kuwayama S, Imai H, Tanabe S, Oda S, Nishida Y, Wada A, Shichida Y, Yamade S. Novel missense mutations in red/green opsin genes in congenital color-vision deficiencies. Biochem. Biophys. Res. Commun. 2002; 294:205–209. [PubMed: 12051694]

Ueyama H, Muraki-Oda S, Yamade S, Tanabe S, Yamashita T, Shichida Y, Ogita H. Unique haplotype in exon 3 of cone opsin mRNA affects splicing of its precursor, leading to congenital color vision defect. Biochem. Biophys. Res. Commun. 2012; 424:152–157. [PubMed: 22732407]

Urich K. Comparative Animal Biochemistry. Springer Science & Business Media. 2013

van den Berg TJTP, Spekreijse H. Near infrared light absorption in the human eye media. Vis. Res. 1997; 37:249–253. [PubMed: 9068825]

Varsanyi B, Somfai GM, Lesch B, Vamos R, Farkas A. Optical coherence tomography of the macula in congenital achromatopsia. Invest. Ophthalmol. Vis. Sci. 2007; 48:2249–2253. [PubMed: 17460287]

Vautier-Giongo C, Bales BL. Estimate of the ionization degree of ionic micelles based on krafft temperature measurements. J. Phys. Chem. B. 2003; 107:5398–5403.

Vogt K, Kirschfeld K. Sensitizing pigment in the fly. Nature. 1983; 9:319–328.

von Lintig J, Kiser PD, Golczak M, Palczewski K. The biochemical and structural basis for trans-to-cis isomerization of retinoids in the chemistry of vision. Trends Biochem. Sci. 2010; 35:400–410. [PubMed: 20188572]

Vorobyev M. Coloured oil droplets enhance colour discrimination. Proc. R. Soc. B Biol. Sci. 2003; 270:1255–1261.

Vorobyev M, Osorio D, Bennett AT, Marshall NJ, Cuthill IC. Tetrachromacy, oil droplets and bird plumage colours. J. Comp. Physiol. A. 1998; 183:621–633. [PubMed: 9839454]

Wald G. On the distribution of vitamins A(1) and A(2). J. General Physiology. 1939a; 22:391–415.

Wald G. The porphyropsin visual system. J. Gen. Physiol. 1939b; 22:775–794. [PubMed: 19873132]

Wald G, Brown PK, Smith PH. Iodopsin. J. General Physiology. 1955; 38:623–681.

Walls, GL. The Vertebrate Eye and its Adaptive Radiation. New York, London: Hafner Publishing Company; 1942.

Wang JS, Kefalov VJ. The cone-specific visual cycle. Prog. Retin Eye Res. 2011; 30:115–128. [PubMed: 21111842]

Wang Y, Macke JP, Merbs SL, Zack DJ, Klaunberg B, Bennett J, Gearhart J, Nathans J. A locus control region adjacent to the human red and green visual pigment genes. Neuron. 1992; 9:429–440. [PubMed: 1524826]

Wang Z, Asenjo AB, Oprian DD. Identification of the Cl(−)-binding site in the human red and green color vision pigments. Biochemistry. 1993; 32:2125–2130. [PubMed: 8443153]

Wang W, Nossoni Z, Berbasova T, Watson CT, Yapici I, Lee KS, Vasileiou C, Geiger JH, Borhan B. Tuning the electronic absorption of protein-embedded all-trans-retinal. Science. 2012; 338:1340–1343. [PubMed: 23224553]

Weitz CJ, Miyake Y, Shinzato K, Montag E, Zrenner E, Went LN, Nathans J. Human tritanopia associated with two amino acid substitutions in the blue-sensitive opsin. Am. J. Hum. Genet. 1992a; 50:498–507. [PubMed: 1531728]

Weitz CJ, Went LN, Nathans J. Human tritanopia associated with a third amino acid substitution in the blue-sensitive visual pigment. Am. J. Hum. Genet. 1992b; 51:444–446. [PubMed: 1386496]

Werner JS, Steele VG. Sensitivity of human foveal color mechanisms throughout the life span. J. Opt. Soc. Am. A. 1988; 5:2122–2130. [PubMed: 3230481]

Wichmann FA, Sharpe LT, Gegenfurtner KR. The contributions of color to recognition memory for natural scenes. J. Exp. Psychol. Learn Mem. Cogn. 2002; 28:509–520. [PubMed: 12018503]

Williams RW. The human retina has a cone-enriched rim. Vis. Neurosci. 1991; 6:403–406. [PubMed: 1829378]

Winderickx J, Battisti L, Motulsky AG, Deeb SS. Selective expression of human X chromosome-linked green opsin genes. Proc. Natl. Acad. Sci. U. S. A. 1992a; 89:9710–9714. [PubMed: 1409688]

Winderickx J, Sanocki E, Lindsey DT, Teller DY, Motulsky AG, Deeb SS. Defective colour vision associated with a missense mutation in the human green visual pigment gene. Nat. Genet. 1992b; 1:251–256. [PubMed: 1302020]

Wong AM, Sharpe JA. Representation of the visual field in the human occipital cortex: a magnetic resonance imaging and perimetric correlation. Arch. Ophthalmol. 1999; 117:208–217. [PubMed: 10037566]

Wright WD. The characteristics of tritanopia. J. Opt. Soc. Am. 1952; 42:509–521. [PubMed: 14946611]

Yamaguchi T, Motulsky AG, Deeb SS. Visual pigment gene structure and expression in human retinae. Hum. Mol. Genet. 1997; 6:981–990. [PubMed: 9215665]

Yamashita T, Nakamura S, Tsutsui K, Morizumi T, Shichida Y. Chloride-dependent spectral tuning mechanism of L-group cone visual pigments. Biochemistry. 2013; 52:1192–1197. [PubMed: 23350963]

Yan ECY, Kazmi MA, Ganim Z, Hou JM, Pan DH, Chang BSW, Sakmar TP, Mathies RA. Retinal counterion switch in the photoactivation of the G protein-coupled receptor rhodopsin. Proc. Natl. Acad. Sci. U. S. A. 2003; 100:9262–9267. [PubMed: 12835420]

Yanagawa M, Kojima K, Yamashita T, Imamoto Y, Matsuyama T, Nakanishi K, Yamano Y, Wada A, Sako Y, Shichida Y. Origin of the low thermal isomerization rate of rhodopsin chromophore. Sci. Rep. 2015; 5:11081. [PubMed: 26061742]

Yau KW, Hardie RC. Phototransduction motifs and variations. Cell. 2009; 139:246–264. [PubMed: 19837030]

Yokoyama S. Molecular evolution of vertebrate visual pigments. Prog. Retin Eye Res. 2000; 19:385–419. [PubMed: 10785616]

Yokoyama S. Evolution of dim-light and color vision pigments. Annu. Rev. Genomics Hum. Genet. 2008; 9:259–282. [PubMed: 18544031]

Yokoyama S, Radlwimmer FB, Blow NS. Ultraviolet pigments in birds evolved from violet pigments by a single amino acid change. Proc. Natl. Acad. Sci. U. S. A. 2000; 97:7366–7371. [PubMed: 10861005]

Yokoyama S, Yang H, Starmer WT. Molecular basis of spectral tuning in the red- and green-sensitive (M/LWS) pigments in vertebrates. Genetics. 2008; 179:2037–2043. [PubMed: 18660543]

Yoshizawa T. Molecular basis for color vision. Biophys. Chem. 1994; 50:17–24. [PubMed: 8011932]

Zalewska M, Siara M, Sajewicz W. G protein-coupled receptors: abnormalities in signal transmission, disease states and pharmacotherapy. Acta Pol. Pharm. 2014; 71:229–243. [PubMed: 25272642]

Zhang T, Enemchukwu NO, Jones A, Wang S, Dennis E, Watt CB, Pugh EN Jr, Fu Y. Genetic deletion of S-opsin prevents rapid cone degeneration in a mouse model of Leber congenital amaurosis. Hum. Mol. Genet. 2015; 24:1755–1763. [PubMed: 25416279]

Zhou X, Sundholm D, Wesolowski TA, Kaila VR. Spectral tuning of rhodopsin and visual cone pigments. J. Am. Chem. Soc. 2014; 136:2723–2726. [PubMed: 24422511]

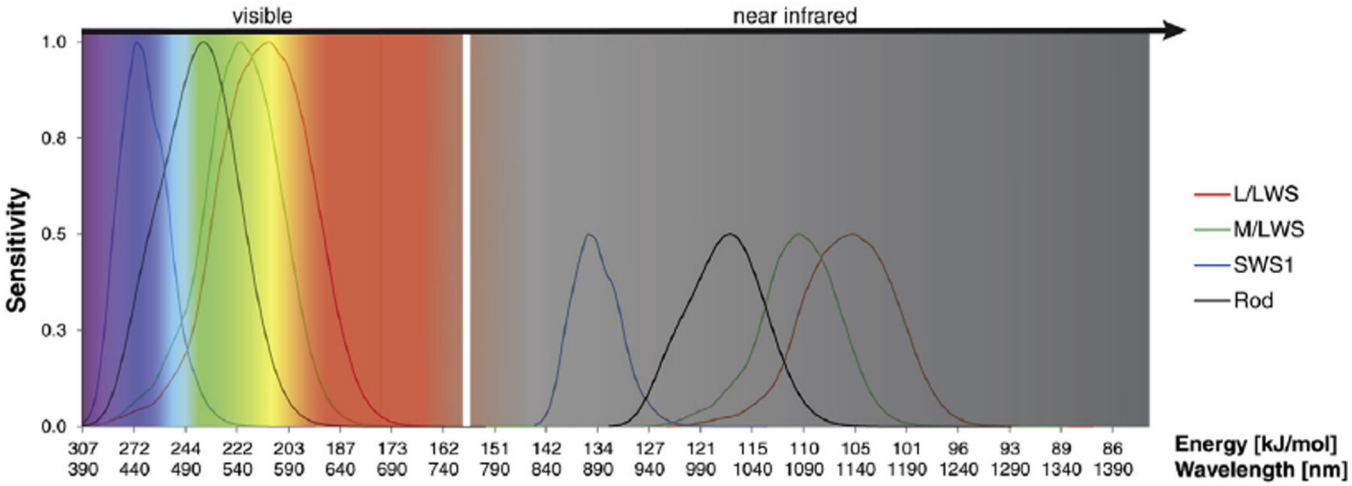

Fig. 1.

Shown are the visible and IR spectra with normalized cone and rod spectral sensitivities according to the 10-deg fundamentals based on the Stiles and Burch 10-deg color matching functions (CMFs) (Stockman and Sharpe, 2000). The normalized sensitivity of the visual spectrum is combined with the corresponding IR spectrum determined by the two-photon effect. The corresponding IR spectrum shows a sensitivity maximum of 50% due to the two-photon effect. The white vertical line separating the classical visible from the near IR spectrum indicates the boundary between these two spectra.

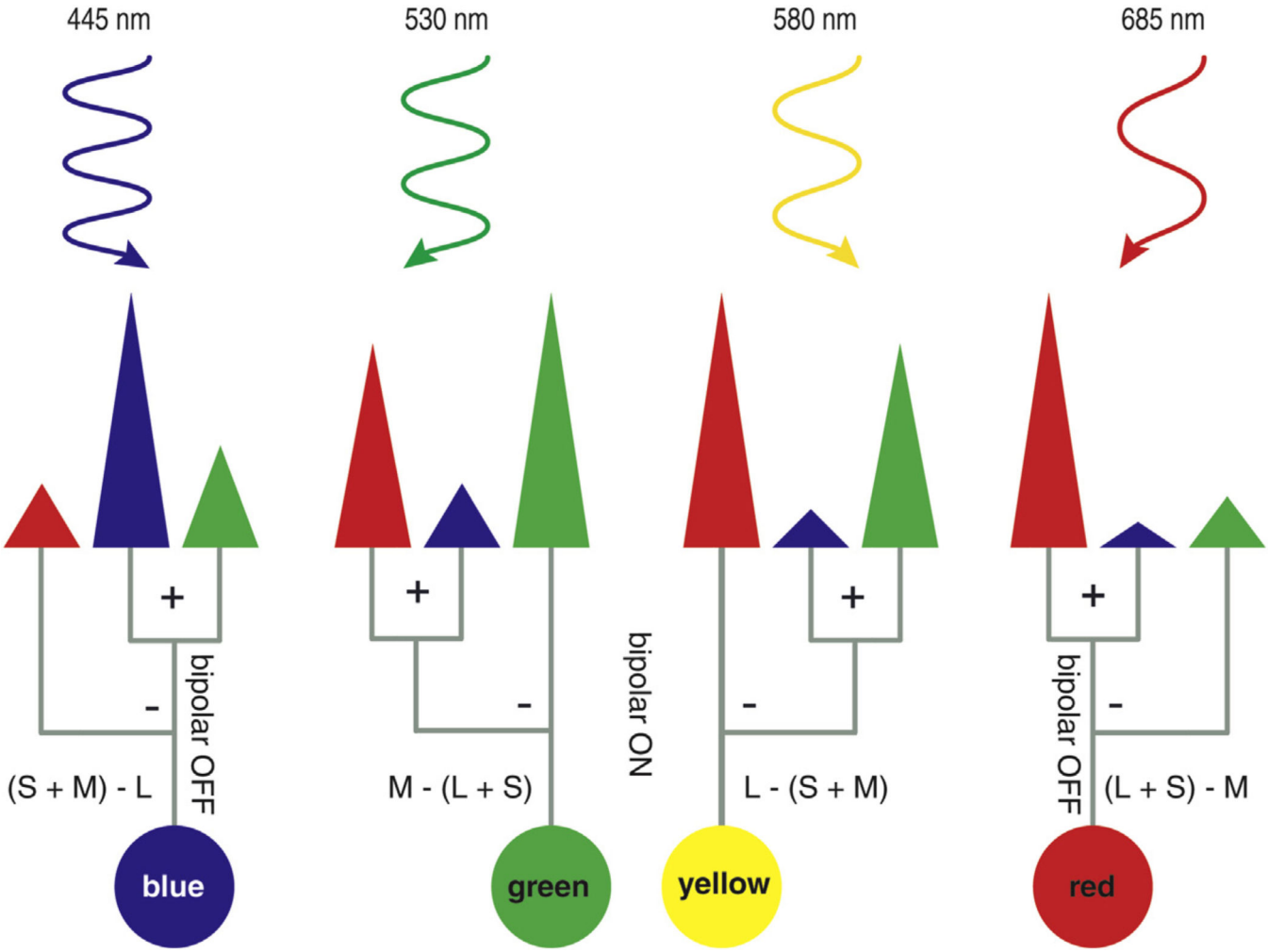

Fig. 2.

A simplified model of light absorption and neuronal processing according to the color opponent theory modified by (Schmidt et al., 2014a). Representations of blue, green, yellow and red monochromatic light from short to long wavelengths are shown at increasing wavelengths. The corresponding qualitative and normalized cone spectral sensitivities are illustrated by the size of each cone. The cones are colored according to their spectral sensitivity, red for L/LWS, green for M/LWS and blue for SWS1 cone photoreceptor cells. A simplified processing of the cone signals through the midget ganglion cells is represented by gray lines which finally results in color perception. Nevertheless, contributions of rod photoreceptor cells and melanopsin containing retinal ganglion cells are still missing (Barrionuevo and Cao, 2014).

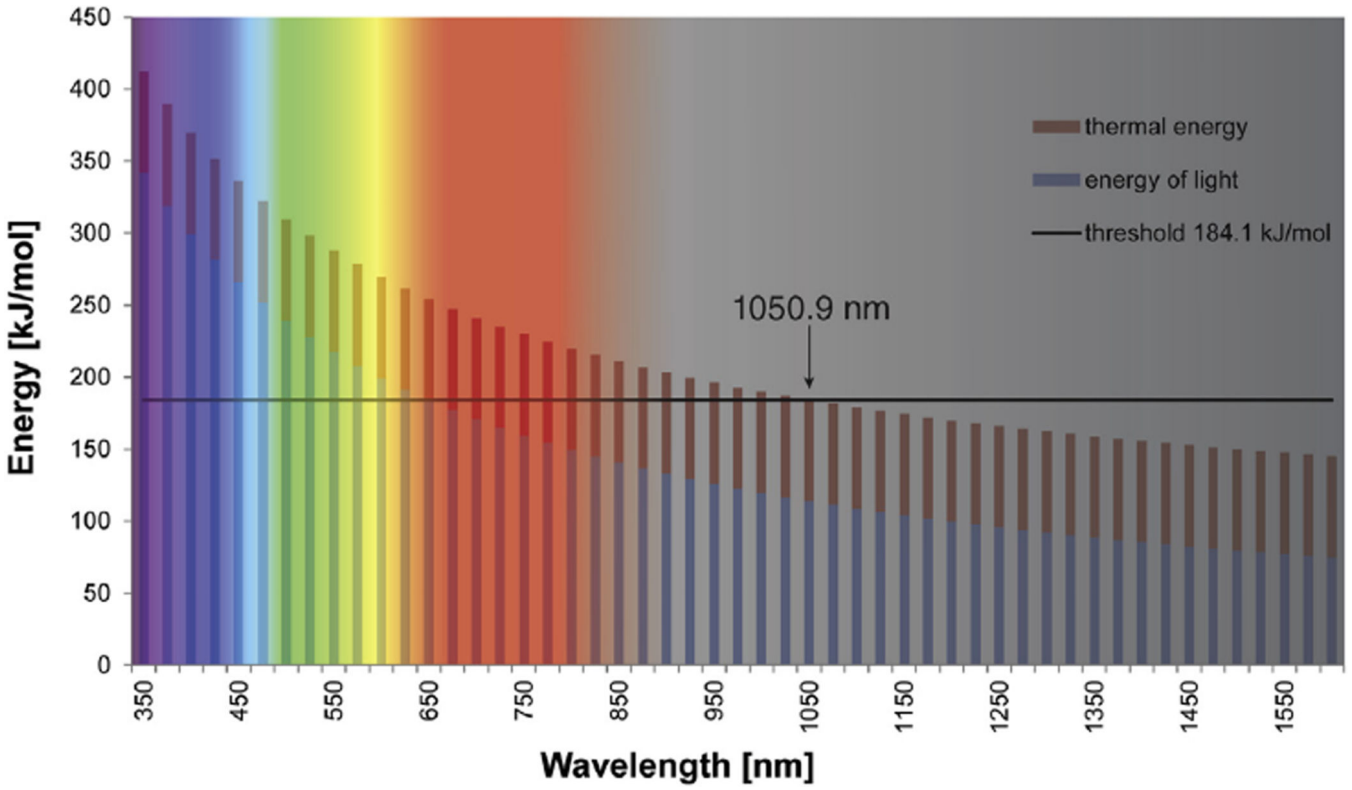

Fig. 3.

Photon specific energy contribution to opsin activation throughout the visible and IR spectra. The wavelength-dependent energy of light is depicted in blue; red bars correspond to the thermal energy contribution of 310.15 K (37 °C), $70.3\frac{kJ}{mol}\left(16.8\frac{kcal}{mol}\right)$. The black horizontal line corresponds to the thermal activation energy of bovine rhodopsin, $E_A^T{=}184.1\frac{kJ}{mol}\left(44.0\frac{kcal}{mol}\right)$ (Lythgoe and Quilliam, 1938). At 1050.9 nm the combined thermal and radiation energy crosses the threshold which implies the theoretical limit of mammalian light perception.

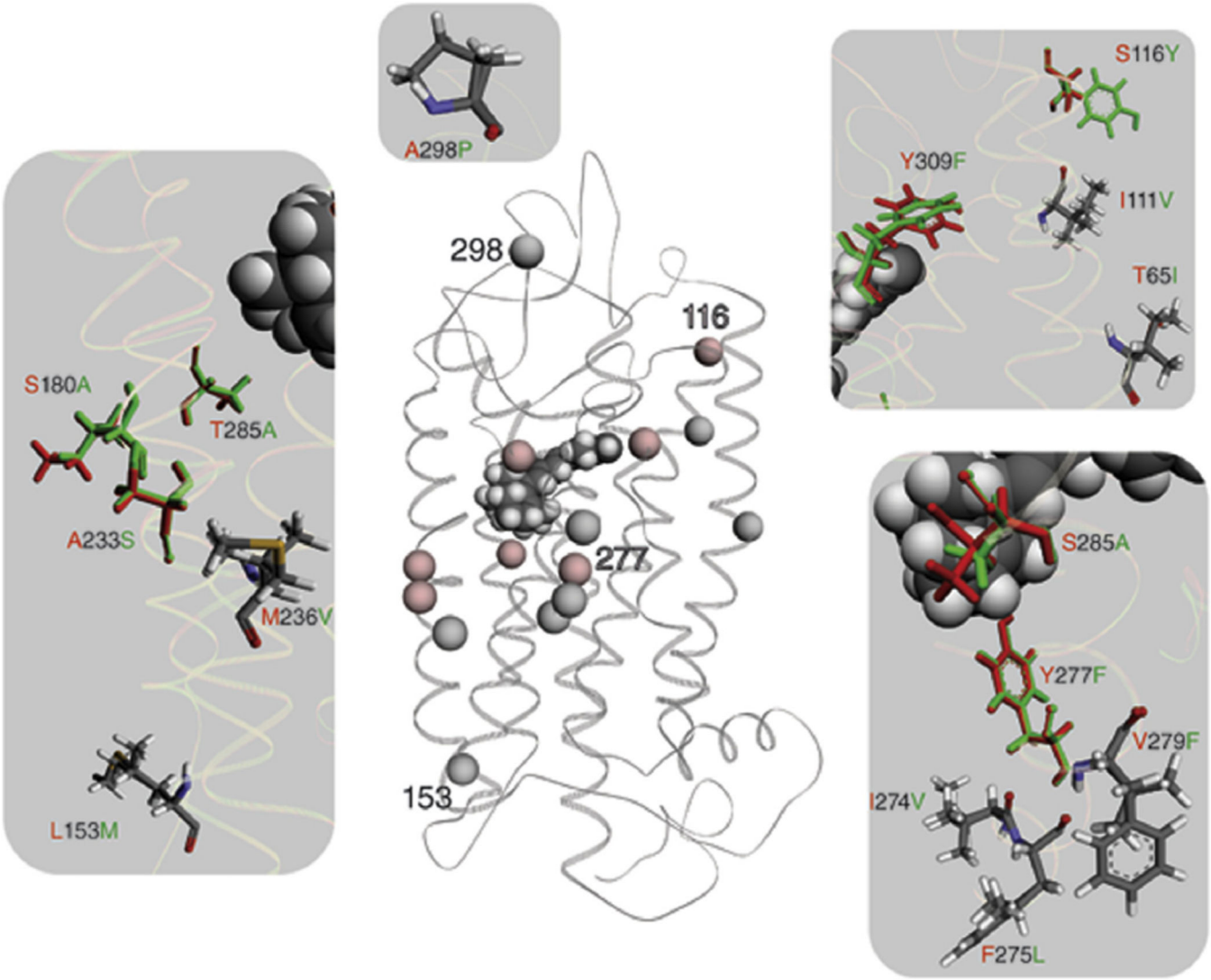

Fig. 4.

A structural comparison between the L/LWS and M/LWS opsin model is shown. Wire representation of the L/LWS and M/LWS model is based on the rhodopsin crystal structure. Spheres illustrate differences in the amino acid sequence between L/LWS and M/LWS. Red spheres indicate differences responsible for spectral tuning between L/LWS and M/LWS, whereas gray spheres do not contribute to color tuning, according to (Asenjo et al., 1994). Numbers within the LWS model help to orient between the magnifications and the GPCR overview. Fifteen changes in amino acid residues are magnified on a gray background; amino acid residues contributing to color tuning are in their corresponding colors, namely red for L/LWS and green for M/LWS. Changed amino acid residues that do not affect spectral tuning are colored according their atoms.

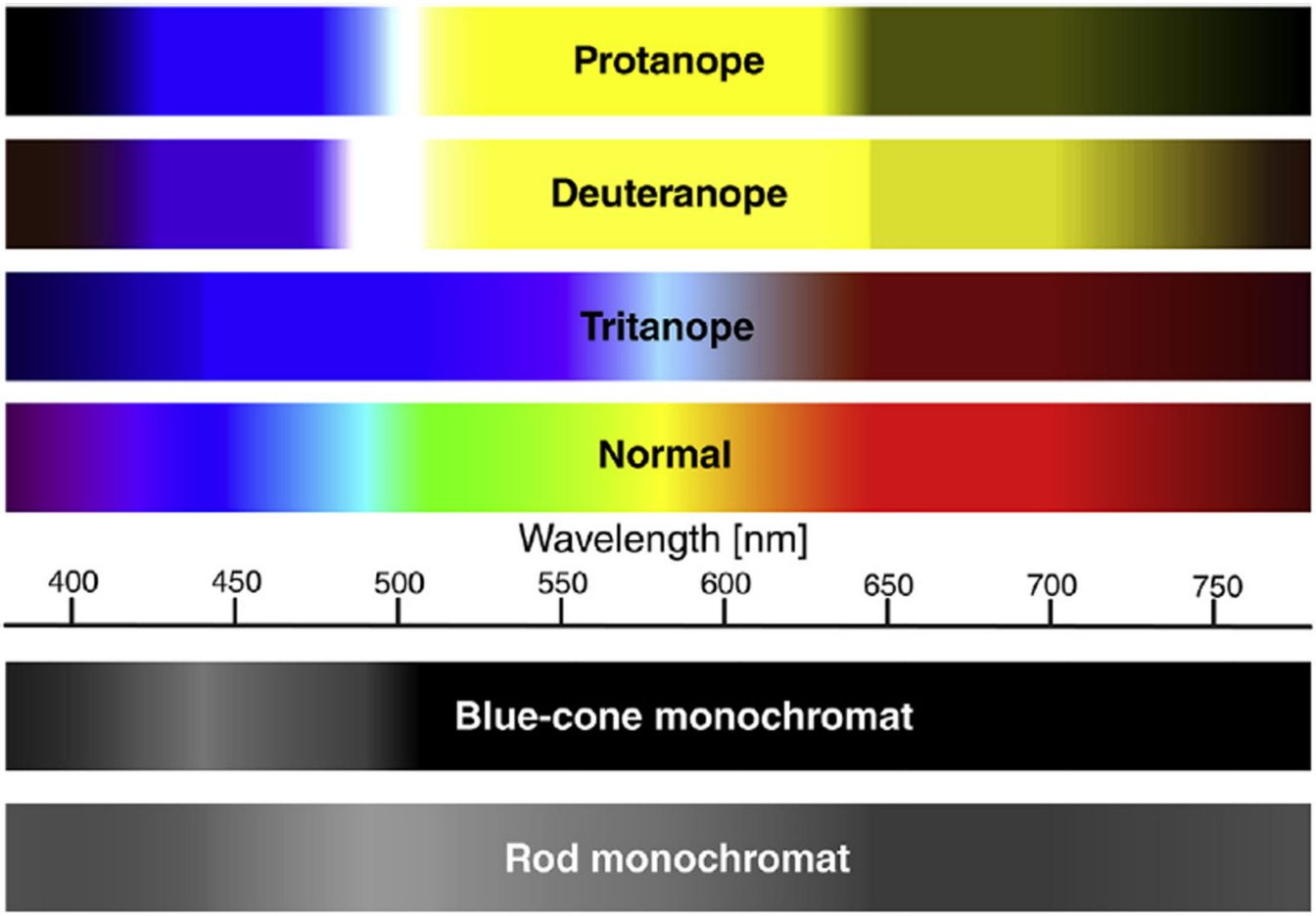

Fig. 5.

Comparison of normal and deficient color vision. Visible spectra illustrated for five types of human color blindness are adapted from (Karl and Gegenfurtner, 2001). The spectra represent only severe cases of color vision deficiencies and a common spectrum for normal color vision. Actually, there are milder degrees of color vision deficiencies such as deuteranomaly and protanomaly. These anomalous trichromats contain at least one normal cone opsin and one set, which evidence a minor spectral shift from each other (Bollinger et al., 2004; Yamaguchi et al., 1997). Furthermore, 38% of Caucasian males with normal trichromacy contain variation in the red opsin that alters the normal spectrum.

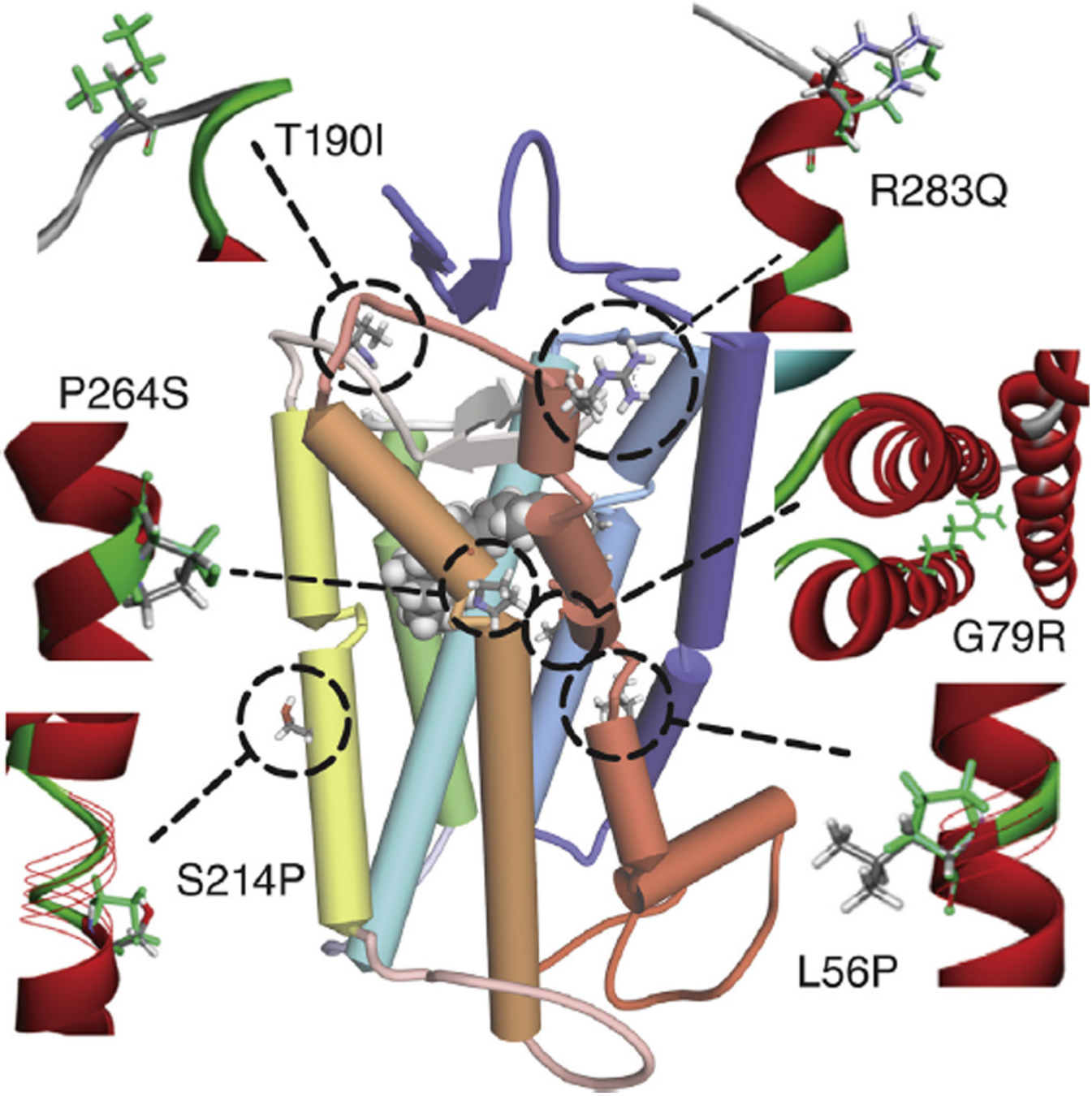

Fig. 6.

A schematic view of the SWS1 opsin with the six disease-causing mutations depicted in black. Each mutation is displayed as green sticks, whereas the wild-type is displayed according to element color. The protein is shown in a ribbon representation colored according to its secondary structure. Red represents α-helical structures, cyan indicates beta strands and loops are shown in green. The structure is displayed as a wire ribbon, where mutations have changed the secondary structure of the wild-type protein.

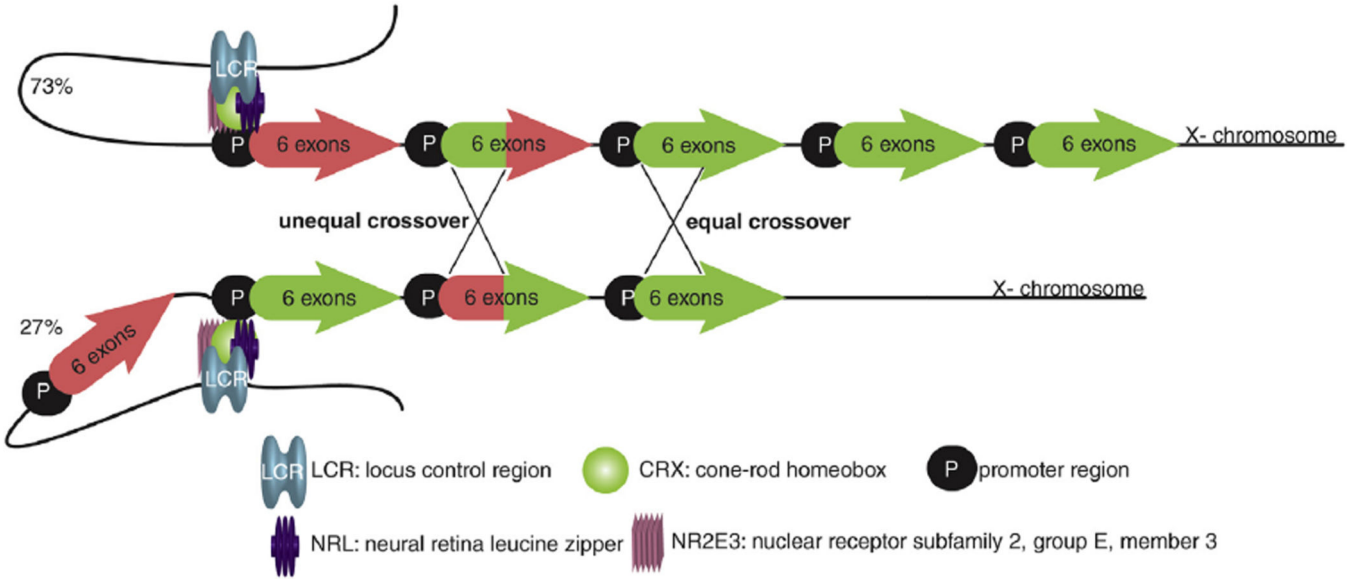

Fig. 7.

A combined figure of transcription regulation, organization and crossover events of LWS opsin genes. L/LWS, M/LWS head to tail gene arrays are shown with the LCR located about 3.5 kb upstream. L/LWS genes are depicted in red, M/LWS genes in green. LCR regulates the expression of the first two LWS gene copies. Obviously a deletion or other damage of the LCR leads to BCM. The left and right crosses indicate unequal or equal crossovers, respectively during meiosis resulting in either a hybrid gene or exchange of a whole gene. The upper strand depicts the binding of LCR to the promoter region of the first L/LWS gene, whereas the lower strand represents the binding of LCR to the first M/LWS gene promoter *via* its three transcription factors. Percentages on the left indicate the distance-dependent probability of gene transcription regulated by LCR in Caucasian males (Carroll et al., 2000; McMahon et al., 2008).

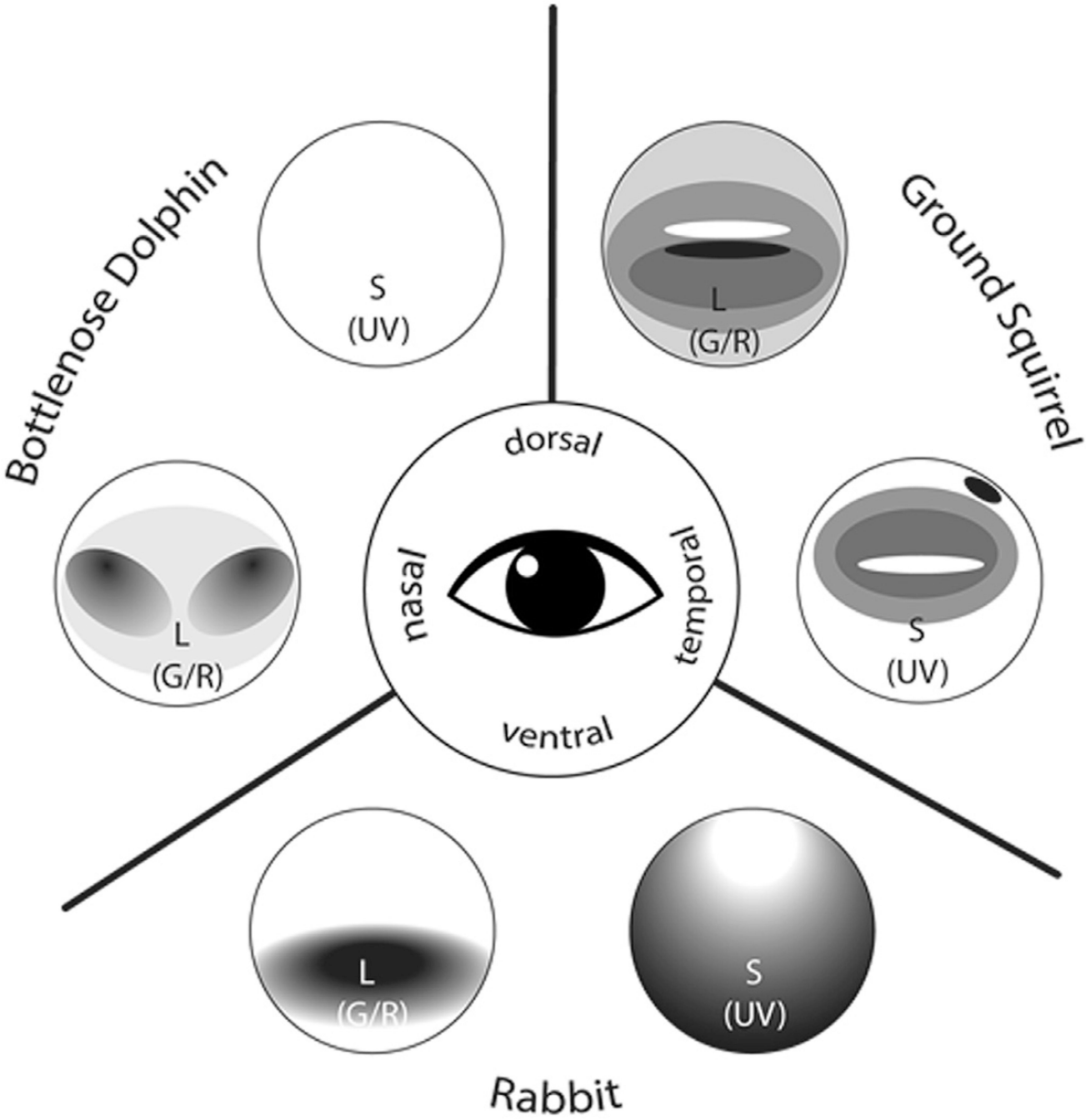

Fig. 8.

Topography of the spectral cone types in mammalian species. The bottlenose dolphin represents marine mammals lacking SWS cone photoreceptor cells. The ground squirrel represents a cone dominant diurnal species with a high density spot of SWS cones in the dorso-temporal region of the retina. The rabbit contains SWS cone photoreceptors in an increasing gradient from the area *centralis* to the ventral region of the retina (Ahnelt and Kolb, 2000).

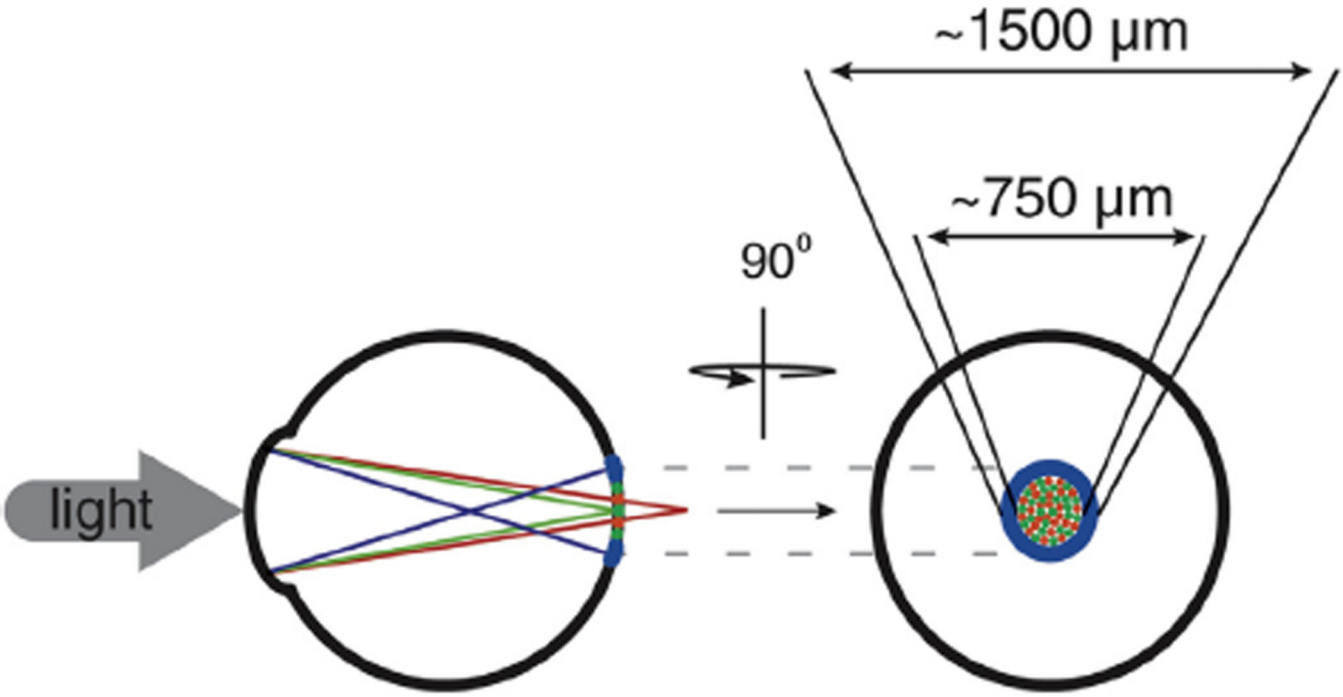

Fig. 9.

Schematic optics of the eye provide an explanation of the SWS1 cone distribution around the central fovea. Polychromatic light indicated by an arrow (left) undergoes different aberrations through the lens and vitreous. This process causes the different focus points behind (red), on (green) and in front (blue) of the retina. Dimensions of fovea are from (Kolb, 2015).

Table 1

A summary of published human opsin absorption maxima (λ_{max}) from 1964 to 2011. Data here show that the absorption maxima are not single values but instead represent an absorption range. This absorption range results from different experimental methods and polymorphisms within the opsins. For simplicity, we have used values published previously (Neitz and Neitz, 2011).

Human Rhodopsin:	λ_{max}	496 nm (Dartnall et al., 1983), 497 nm (Bowmaker and Dartnall, 1980), 505 nm (Brown and Wald, 1964), 498 nm (Nathans, 1990).
Human SWS1:	λ_{max}	426 nm (Merbs and Nathans, 1992), 424 nm (Oprian et al., 1991), 419 nm (Dartnall et al., 1983), 410 nm (Asenjo et al., 1994), 420 nm (Bowmaker and Dartnall, 1980), 450 nm (Brown and Wald, 1964), 420 nm (Neitz and Neitz, 2011).
Human M/LWS:	λ_{max}	530 nm (Merbs and Nathans, 1992), 530 nm (Oprian et al., 1991), 530 nm (Dartnall et al., 1983), 532 nm (Asenjo et al., 1994), 533 nm (Bowmaker and Dartnall, 1980), 525 nm (Brown and Wald, 1964), 530 nm (Neitz and Neitz, 2011).
Human L/LWS:	λ_{max}	552 nm (Merbs and Nathans, 1992), 560 nm (Oprian et al., 1991), 558 nm (Dartnall et al., 1983), 563 nm (Asenjo et al., 1994), 562 nm (Bowmaker and Dartnall, 1980), 555 nm (Brown and Wald, 1964), 557.5 nm (Neitz and Neitz, 2011).
Human melanopsin	λ_{max}	*479 nm* (Bailes and Lucas, 2013)

Table 2

Conversion of specific absorption maxima (λ_{max}) into corresponding energy units (Neitz and Neitz, 2011).

	Wavelength (λ_{max})	**Energy (E)**[a]					
	[nm]	**[*kJ/mol*]**	**[*kcal/mol*]**	**[10^{-19} J]**	**[10^{-20} cal]**	**[eV]**	**[cm^{-1}]**
Rhodopsin	498 nm	240.21	57.41	3.98	9.53	2.49	20,080.32
SWS1	420 nm	284.83	68.07	4.73	11.30	2.95	23,809.51
M/LWS	530 nm	225.71	53.95	3.75	8.95	2.34	18,867.88
L/LWS	557.5 nm	214.58	51.29	3.56	8.51	2.22	17,937.48
Melanopsin	479 nm	249.74	59.69	4.15	9.91	2.58	20,876.88

[a]Calculated from: $E = h{\cdot}c/\lambda_{max}$; c = 299792458 m/s; h = 6:62606957(29)$\cdot 10^{-34}$ Js.

Table 3

Disease causing mutations in LWS and SWS1 opsin genes.

Opsin	Mutation	Phenotype
L/LWS and M/LWS[a]	N94K (Ueyama et al., 2002)	deutan
	C203R (Winderickx et al., 1992b), (Nathans et al., 1993)	deutan, or BCM if both L/LWS and M/LWS are affected
	W177R (Gardner et al., 2010)	X-linked cone-rod dystrophy
	R247Ter (Nathans et al., 1993)	BCM with single L/LWS opsin gene
	P307L (Nathans et al., 1993)	BCM with a single L/LWS-M/LWS hybrid gene
	R330N (Ueyama et al., 2002)	deutan
	G338E (Ueyama et al., 2002)	protan, deutan
	L/M153, I/V171, A174, V178 and A/S180 (LIAVA, LVAVA, LIAVS or MIAVA) (Carroll et al., 2004; Gardner et al., 2014; Mizrahi-Meissonnier et al., 2010; Neitz et al., 2004; Ueyama et al., 2012)	protan, deutan
SWS1	G79R (Weitz et al., 1992a)	tritan
	L56P (Gunther et al., 2006)	tritan
	T190I (Baraas et al., 2012)	mild tritan (at high luminance), severe tritan (at low luminance)
	S214P (Weitz et al., 1992a)	tritan
	P264S (Weitz et al., 1992a)	tritan
	R283Q (Baraas et al., 2007)	tritan, SWS1 cone degeneration

[a]Mutations in L/LWS and M/LWS can cause similar impairments because high homology between these two pigments and thus are grouped together.

Table 4

Classification of oil droplet types based on carotenoid content.

Type[a]	Visual appearance	Always present	λ_{max} [nm]	Number of carotenoids
R	Red	+	477 ± 2.3	1
O	Orange	−	425–477	1–2
Y	Yellow	+	435–455	1–2
P	Pale yellow or greenish	+	375–455	2
C_J	Colorless (or pale yellow)	+	375–405	1
C_S	Colorless (or pale yellow)	−	375–405	1
T_J	Transparent	−	None	0
T_S	Transparent	+	None	0

[a]Lower case ‘j’ and ‘s’ indicate the relative size of the droplet, with ‘j’ representing the small and ‘s’ the large size. Adapted from (Goldsmith et al., 1984).